

6-2022

USING METAL-ORGANIC FRAMEWORKS (MOF) TO REDUCE THE CARBON FOOTPRINT OF CONCRETE

Mona Ibrahim El-Hallak
United Arab Emirates University

Follow this and additional works at: https://scholarworks.uaeu.ac.ae/all_theses



Part of the [Civil Engineering Commons](#), and the [Environmental Engineering Commons](#)

Recommended Citation

El-Hallak, Mona Ibrahim, "USING METAL-ORGANIC FRAMEWORKS (MOF) TO REDUCE THE CARBON FOOTPRINT OF CONCRETE" (2022). *Theses*. 1149.
https://scholarworks.uaeu.ac.ae/all_theses/1149

This Thesis is brought to you for free and open access by the Electronic Theses and Dissertations at Scholarworks@UAEU. It has been accepted for inclusion in Theses by an authorized administrator of Scholarworks@UAEU. For more information, please contact mariam_aljaberi@uaeu.ac.ae.



MASTER THESIS NO. 2022: 36

College of Engineering

Department of Civil and Environmental Engineering

**USING METAL-ORGANIC FRAMEWORKS (MOF) TO REDUCE
THE CARBON FOOTPRINT OF CONCRETE**

Mona Ibrahim El-Hallak



June 2022

United Arab Emirates University

College of Engineering

Department of Civil and Environmental Engineering

USING METAL-ORGANIC FRAMEWORKS (MOF) TO REDUCE
THE CARBON FOOTPRINT OF CONCRETE

Mona Ibrahim El-Hallak

This thesis is submitted in partial fulfilment of the requirements for the degree of Master
of Science in Civil Engineering

June 2022

United Arab Emirates University Master Thesis
2022: 36

Cover: Image related to the incorporation of metal-organic frameworks (MOF) in concrete used in the research

(Photo: By Mona Ibrahim El-Hallak)


© 2022 Mona Ibrahim El-Hallak, Al Ain, UAE

All Rights Reserved

Print: University Print Service, UAEU 2022

Declaration of Original Work

I, Mona Ibrahim El-Hallak, the undersigned, a graduate student at the United Arab Emirates University (UAEU), and the author of this thesis entitled “*Using Metal-Organic Frameworks (MOF) to Reduce the Carbon Footprint of Concrete*”, hereby, solemnly declare that this is the original research work that has been done and prepared by me under the supervision of Dr. Hilal El-Hassan, in the College of Engineering at UAEU. This work has not previously formed the basis for the award of any academic degree, diploma or a similar title at this or any other university. Any materials borrowed from other sources (whether published or unpublished) and relied upon or included in my thesis have been properly cited and acknowledged in accordance with appropriate academic conventions. I further declare that there is no potential conflict of interest with respect to the research, data collection, authorship, presentation and/or publication of this thesis.

Student's Signature: 

Date: 29.4.2022

Advisory Committee

1) Advisor: Dr. Hilal El-Hassan

Title: Associate Professor

Department of Civil and Environmental Engineering

College of Engineering

2) Co-advisor: Prof. Amr S. El-Dieb

Title: Professor

Department of Civil and Environmental Engineering

College of Engineering

3) Co-advisor: Dr. Ahmed Alzamly


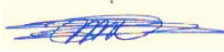

Title: Associate Professor

Department of Chemistry

College of Science

Approval of the Master Thesis

This Master Thesis is approved by the following Examining Committee Members:

- 1) Advisor (Committee Chair): Dr. Hilal El-Hassan
Title: Associate Professor
Department of Civil and Environmental Engineering
College of Engineering
Signature  Date June 27, 2022
- 2) Member: Dr. Bilal El-Ariss
Title: Associate Professor
Department of Civil and Environmental Engineering
College of Engineering
Signature  Date June 27, 2022
- 3) Member (External Examiner): Dr. Ahmed Soliman
Title: Associate Professor
Department of Building, Civil, and Environmental Engineering
Institution: Concordia University, Canada
Signature  On behalf of Date June 27, 2022

This Master Thesis is accepted by:

Acting Dean of the College of Engineering: Professor Mohamed Al-Marzouqi

Signature Mohamed AlMarzouqi

Date July 14, 2022

Dean of the College of Graduate Studies: Professor Ali Al-Marzouqi

Signature Ali Hassan

Date July 14, 2022

Abstract

The production of concrete by the construction industry has a massive impact on the environment. The process of manufacturing its main component, cement, releases a considerable amount of anthropogenic carbon dioxide. This thesis is concerned with the production of sustainable and eco-friendly concrete that integrates metal-organic frameworks (MOF) to capture and offset the CO₂ emissions emitted during the production of cement. The main objective is to synthesize a MOF capable of capturing CO₂ in concrete through accelerated carbonation curing and to assess its impact on concrete performance. Different parameters were examined, including the MOF content, initial curing duration, and carbonation curing duration and pressure. The parameters were evaluated through CO₂ uptake, phenolphthalein indicator solution, compressive strength, water absorption, and permeable pore voids volume. The microstructure of carbonated MOF-incorporating concrete was evaluated using powder X-ray diffraction analysis, scanning electron microscope, and Fourier transform infrared spectroscopy. The study revealed the possibility of incorporating MOF in concrete to capture CO₂ gas, permanently sequester it, and increase CO₂ uptake while either improving or not impacting the concrete performance. The addition of MOF promoted a higher carbonation degree of cement, especially with a longer initial curing duration and higher pressures. Incorporating up to 6% MOF, by cement mass, in concrete mix cured for 20 hours in open-air followed by 20 hours of carbonation curing at a pressure of 1 bar led to the highest total CO₂ uptake of 19%, carbonation depth of 11 mm, and 28-day strength of 46 MPa. Meanwhile, its water absorption and permeable pore voids volume were the lowest at 4 and 11%, respectively. Exceeding 6% MOF addition did not seem to improve the uptake or performance. In comparison, the carbonated control mix without the MOF showed lower compressive strength and higher porosity. Furthermore, the microstructure analysis highlighted the formation of calcite, aragonite, calcium silicate hydrate, calcium hydroxide, and ettringite. The developed MOF-incorporating concrete can be used in construction applications to mitigate the industry-related CO₂ emissions while maintaining concrete properties.

Keywords: CO₂ emissions, metal-organic framework, MOF, concrete, cement, accelerated carbonation, curing, pressure, CO₂ uptake, performance, microstructure.

Title and Abstract (in Arabic)

استخدام الهياكل الفلزية العضوية (MOF) لتقليل البصمة الكربونية للخرسانة

الملخص

الإنتاج الهائل من الخرسانة في مجال البناء له تأثير كبير على البيئة. تؤدي عملية صناعة مكونه الرئيسي، الإسمنت، إلى انبعاث كمية كبيرة من ثاني أكسيد الكربون. تهتم هذه الأطروحة بإنتاج خرسانة مستدامة صديقة للبيئة تستخدم الهياكل الفلزية العضوية (MOF) لالتقاط وتعويض انبعاثات ثاني أكسيد الكربون الناتجة من عملية إنتاج الإسمنت. الهدف الرئيسي هو إنشاء هيكل فلزي عضوي قادر على التقاط ثاني أكسيد الكربون داخل الخرسانة عن طريق المعالجة الكربونية المتسارعة وتقييم تأثيرها على خصائص الخرسانة. تم دراسة عوامل مختلفة تشمل كمية الهيكل الفلزي العضوي، مدة المعالجة الأولية، فترة الكربنة المعجلة والضغط. تم تقييم هذه العوامل عن طريق كمية امتصاص ثاني أكسيد الكربون، محلول الفينول فتالين، قوة الضغط، امتصاص الماء وحجم الفراغات المسامية. تم تقييم البنية المجهرية للخرسانة التي تحتوي على MOF والمعرضة لعملية الكربنة عن طريق تحليل حيود الأشعة السينية، مجهر المسح الإلكتروني وتحويل فورييه الطيفي بالأشعة تحت الحمراء. أظهرت الدراسة إمكانية استخدام الهياكل الفلزية العضوية في الخرسانة لاحتجاز غاز ثاني أكسيد الكربون وعزله بشكل دائم وزيادة امتصاص ثاني أكسيد الكربون مع تحسين أداء الخرسانة أو عدم التأثير عليه. إن إضافة الهياكل الفلزية العضوية زادت من درجة الكربنة للإسمنت، خصوصاً مع فترة أطول للمعالجة الأولية وضغط أعلى. أدى إضافة الهياكل الفلزية العضوية (MOF) بنسبة تصل إلى 6%، من وزن الإسمنت، إلى مزيج الخرسانة تحت 20 ساعة معالجة أولية يتبعها 20 ساعة كربنة معجلة تحت ضغط مساوي ل 1 bar إلى أعلى نسبة امتصاص لثاني أكسيد الكربون تساوي 19%، عمق كربنة يساوي 11 mm وأعلى قوة ضغط مساوية ل 46 MPa في عمر 28 يوماً. وفي الوقت نفسه، نسبة امتصاص الماء وحجم الفراغات المسامية كانت الأدنى وتساوي 4% و 11%، على التوالي. إضافة الهياكل الفلزية العضوية بنسبة تتجاوز 6% لم تؤدي إلى تحسين امتصاص ثاني أكسيد الكربون أو خصائص الخرسانة. في المقابل، أظهر مزيج الخرسانة الذي لا يحتوي على هياكل فلزية عضوية والمعرض للكربنة المعجلة قوة ضغط أقل ومسامية أعلى. علاوة على ذلك، أظهر تحليل البنية المجهرية لمخاليط مختلفة تكون الكالسييت، أراجونيت، هيدرات سيليكات الكالسيوم، هيدروكسيد الكالسيوم و إترينجيت. يمكن استخدام الخرسانة المطورة التي تحتوي على MOF في تطبيقات البناء للتخفيف من انبعاثات ثاني أكسيد الكربون مع الحفاظ على خصائص الخرسانة. كما تم ذكر قيود الدراسة والتوصيات المستقبلية لتوفير أفضل فهم للخرسانة المطروحة.

مفاهيم البحث الرئيسية: انبعاثات ثاني أكسيد الكربون، الهياكل الفلزية العضوية، MOF، الخرسانة، الإسمنت، الكربنة المعجلة، المعالجة الأولية، الضغط، كمية امتصاص ثاني أكسيد الكربون، الأداء، البنية المجهرية.

Author Profile

Mona Ibrahim El-Hallak is a Master thesis student in the civil and environmental engineering department at the United Arab Emirates University, UAE. She completed her bachelor's degree with a grade of excellent in the same specialty from UAEU. Currently, she is working as a research assistant in the concrete technology area. She has also worked as a teaching assistant at the university. Mona has more than two years of experience in advising undergraduate students. She has been awarded by the academic advising unit in the UAEU for her hard work and achievements. In 2017, Mona was also awarded by the United Arab Emirates University for excellence. She received another award from the civil and environmental engineering student society (CEESS) for being an active member in 2018. Mona has attended many workshops. In addition, she has organized and presented two workshops titled "Graduation project" and "Industrial training experience". Mona lives in Al Ain with her family. She was born on February 26th, 1995. Her personal interests are reading, drawing, and writing.

Acknowledgements

I would like to express my special and deepest thanks of gratitude and appreciation to my advisor Dr. Hilal El-Hassan for his endless guidance, continuous support, invaluable advice, and patient supervision throughout all the preparation stages of this thesis study. He generously gave his time to offer me valuable comments about improving my work. Without his constant willingness to share his vast information, knowledge, and suggestions, I would not have made headway in the research.

My sincere thanks must also extend to my co-advisors, Prof. Amr S. El-Dieb and Dr. Ahmed Alzamly, for their valuable cooperation, encouragement, and assistance in various phases of the completion of the project.

There are no proper words to convey my deep gratitude for my family for their unfailing emotional support, unconditional trust, endless patience, and timely encouragement despite the long duration. It was them who raised me up again when I got weary. I would like to thank them for believing in me and motivating me during the hard times that I have faced over the years. There is no way to express how much it meant to me.

Deep gratitude also goes to my best friend, great companion, and husband, Dr. Sarmad, for his endless patience, support, encouragement, and understanding. He went with me through this journey, cheered me on, and celebrated each achievement I have reached. I would like to thank him for trusting me, believing in me, and being proud of me in every step I have made in the research.

I would like to thank Mr. Faisal Abdul Wahab and Eng. Abdelrahman Alsallamin for their great help and support during my work in the concrete laboratory over the thesis duration.

Dedication

To my beloved family and husband

Table of Contents

Title.....	i
Declaration of Original Work.....	iii
Advisory Committee.....	iv
Approval of the Master Thesis	v
Abstract.....	vii
Title and Abstract (in Arabic).....	viii
Author Profile	ix
Acknowledgements.....	x
Dedication.....	xi
Table of Contents.....	xii
List of Tables	xiv
List of Figures.....	xv
List of Abbreviations	xvii
Chapter 1: Introduction.....	1
1.1 Overview	1
1.2 Research Objectives	1
1.3 Relevant Literature	2
1.3.1 Background on Portland Cement.....	2
1.3.2 Mitigation Techniques of CO ₂ Emissions from Cement Production.....	3
1.3.3 Metal-Organic Frameworks.....	12
1.4 Outline and Organization of Thesis	13
1.5 Research Significance	14
Chapter 2: Experimental Program	15
2.1 Overview	15
2.2 Test Program	15
2.3 Materials.....	17
2.4 Methodology	21
2.4.1 Metal-Organic Frameworks (MOFs) Synthesis and Activation.....	21
2.4.2 Concrete Mix Proportions.....	23
2.4.3 Concrete Sample Preparation.....	24
2.4.4 Curing Regimes	25

2.4.5 Carbon Uptake	27
2.4.6 Phenolphthalein Carbonation Indicator	28
2.4.7 Concrete Performance Evaluation	28
2.4.8 Microstructure Characterization	31
Chapter 3: Results and Discussions – Concrete Performance	34
3.1 Overview	34
3.2 Carbon Uptake.....	34
3.2.1 Effect of Quantity of MOF	35
3.2.2 Effect of Initial Curing Duration	38
3.2.3 Effect of Accelerated Carbonation Duration	39
3.2.4 Effect of CO ₂ Pressure	40
3.3 Phenolphthalein Solution Evaluation	41
3.4 Compressive Strength	43
3.4.1 Effect of MOF Quantity	45
3.4.2 Effect of Initial Curing Duration	46
3.4.3 Effect of Accelerated Carbonation Curing Duration	47
3.4.4 Effect of CO ₂ Pressure	48
3.5 Water Absorption and Permeable Pore Voids Volume.....	48
Chapter 4: Results and Discussion – Microstructural Characterization	52
4.1 Overview	52
4.2 Experimental Results.....	52
4.2.1 Powder X-ray Diffraction (PXRD) Analysis.....	52
4.2.2 Scanning Electron Microscope (SEM)	55
4.2.3 Fourier Transform Infrared (FTIR) Spectroscopy	64
Chapter 5: Conclusion	67
5.1 Overview	67
5.2 Limitations of Work	67
5.3 Main Findings and Conclusions	68
5.4 Recommendations for Future Studies	70
References.....	71

List of Tables

Table 1: Experimental test matrix	16
Table 2: Chemical composition of cement	17
Table 3: Physical properties of crushed limestone aggregates	18
Table 4: Mix proportions of trial concrete mixes	24
Table 5: Trial control mixes properties	24
Table 6: Comparison of CO ₂ uptake obtained from mass gain and TDA	34
Table 7: Carbonation reaction measurements of concrete mixes	37
Table 8: Average carbonation depths of concrete mixes at 28 days	43
Table 9: Strength gain of concrete over time	45
Table 10: Water absorption and permeable pore voids volume at 28 days.....	49

List of Figures

Figure 1: SEM micrograph of OPC	17
Figure 2: Sieve analysis of crushed limestone aggregates	18
Figure 3: FTIR spectra of crushed limestone aggregates	19
Figure 4: PXRD pattern of NH ₂ -MIL-125 (Ti)	20
Figure 5: SEM micrograph of NH ₂ -MIL-125 (Ti)	20
Figure 6: FTIR spectrum of MOF, NH ₂ -MIL-125 (Ti)	21
Figure 7: NH ₂ -MIL-125 (Ti) synthesis.....	22
Figure 8: NH ₂ -MIL-125 (Ti) filtration and washing	22
Figure 9: NH ₂ -MIL-125 (Ti) activation.....	23
Figure 10: Trial control mixes	23
Figure 11: Concrete mixes after casting and curing	25
Figure 12: Open-air curing of concrete samples	25
Figure 13: Carbonation setup	26
Figure 14: Schematic diagram of carbonation setup	26
Figure 15: Post-carbonation curing techniques	27
Figure 16: Compressive strength test machine.....	29
Figure 17: Tested cubes for compressive strength	29
Figure 18: Oven-dried specimens for water absorption	30
Figure 19: Immersed cubes for water absorption	30
Figure 20: Boiled samples for permeable voids pore volume	31
Figure 21: Suspended cubes for permeable voids pore volume	31
Figure 22: Prepared samples for SEM.....	32
Figure 23: FTIR spectrometer	33
Figure 24: Interground sample with potassium bromide for FTIR	33
Figure 25: Carbon uptake percent by cement mass for concrete mixes	35
Figure 26: Carbon uptake by cement mass as a function of MOF content	36
Figure 27: Carbon uptake by cement mass as a function of initial curing duration.....	39
Figure 28: Carbon uptake by cement mass as a function of carbonation curing duration.....	40
Figure 29: Carbon uptake by cement mass as a function of carbonation pressure	41
Figure 30: Images of samples sprayed with phenolphthalein indicator solution	42
Figure 31: Compressive strength of concrete mixes	44
Figure 32: Correlation between 28-day compressive strength and each of water absorption and permeable pore volume.....	50
Figure 33: Correlation between carbon uptake by cement mass and each of water absorption and permeable pore volume.....	51
Figure 34: PXRD patterns of concrete at 1 day.....	54

Figure 35: PXRD patterns of concrete at 28 days	55
Figure 36: SEM of 1-day hydrated control mix C0.....	56
Figure 37: SEM of 1-day carbonated mix C1.....	56
Figure 38: EDX analysis of point 1 in mix C1	57
Figure 39: SEM of 1-day mix M1-2	57
Figure 40: EDX analysis of point 1 in mix M1-2.....	58
Figure 41: SEM of 28-day hydrated control mix C0.....	58
Figure 42: SEM of 28-day carbonated mix C4.....	59
Figure 43: EDX analysis of point 1 in mix C4	59
Figure 44: SEM of 28-day carbonated mix M4.....	60
Figure 45: EDX analysis of point 1 in mix M4	60
Figure 46: SEM of 28-day carbonated mix M2.....	61
Figure 47: SEM of 28-day carbonated mix M1-2	61
Figure 48: EDX analysis of point 1 in mix M1-2.....	62
Figure 49: SEM of 28-day carbonated mix M3.....	62
Figure 50: EDX analysis of point 1 in mix M3	63
Figure 51: SEM of 28-day carbonated mix M4 after spraying	64
Figure 52: EDX analysis of point 1 in mix M4 after spraying.....	64
Figure 53: FTIR spectra of the 1-day samples	66
Figure 54: FTIR spectra of the 28-day samples	66

List of Abbreviations

a	Initial Curing Duration
AM	Apparent Mass
AOD	Argon-Oxygen Decarburization Slag
ASTM	American Society for Testing and Materials
BET	Brunauer, Emmett and Teller
BM	Saturated Surface Dry Mass After Boiling
BS	British Standards
c	Carbonation Curing Duration
C ₂ S	Dicalcium Silicate
C ₃ S	Tricalcium Silicate
CaCO ₃	Calcite
CaO	Lime
C-A-S-H	Calcium Aluminosilicate Hydrate
CCUS	Carbon Dioxide Capture, Utilization, and Storage
CG	Coal Gangue
CMUs	Concrete Masonry Units
CO ₂	Carbon Dioxide
C-S-H	Calcium Silicate Hydrate
DCM	Dichloromethane
DMF	N,N-Dimethylformamide
ECC	Engineered Cementitious Composite
EDX	Energy-Dispersive X-ray
EF	Engineered Fuel
f _c	Compressive Strength

FA	Fly Ash
FTIR	Fourier Transform Infrared
GGBFS	Ground Granulated Blast-Furnace Slag
GHG	Greenhouse Gases
GPC	Geopolymer Concrete
HVFA	High-Volume Fly Ash
IEAGHG	International Energy Agency Greenhouse Gas
ITZ	Interfacial Transition Zone
KBr	Potassium Bromide
LCA	Life Cycle Assessment
MBM	Meat and Bone Meal
MgO	Magnesium Oxide
MKG	Metakaolin-Based Geopolymer
MOF	Metal-Organic Frameworks
MRFs	Material Recovery Facilities
MSW	Municipal Solid Waste
NRPP	Non-Recycled Plastics and Paper Residue
OD	Oven-Dried Mass
OPC	Ordinary Portland Cement
PLC	Portland Limestone Cement
PXRD	Powder X-ray Diffraction Analysis
s	Spraying
SCMs	Supplementary Cementitious Materials
SEM	Scanning Electron Microscope
SF	Silica Fume
SRF	Solid Recovered Fuel

SSD	Saturated Surface Dry Mass
TDA	Thermal Decomposition Analysis
UHPC	Ultra-High Performance Concrete
VA	Volcanic Ash
WAAC	Waste Autoclaved Aerated Concrete
WDF	Wood Derived Fuel
XRF	X-ray Fluorescence
ρ	Density

Chapter 1: Introduction

1.1 Overview

The ever-increasing level of carbon dioxide (CO₂) emissions to the atmosphere is a pressing contemporary environmental and ecological concern. The construction industry is responsible for a significant amount of these anthropogenic emissions through the production of concrete and its main binder component, cement.

To this end, researchers have investigated different methods to reduce CO₂ emissions associated with the manufacture and use of cement in concrete. Several measures to mitigate these emissions have been developed and implemented, such as the substitution of fossil fuels with a lower-carbon content fuel, carbon dioxide capture, utilization, and storage (CCUS), and partial and full replacement of cement by supplementary cementitious materials (SCMs). Despite providing promising results to alleviate the carbon dioxide emissions, the before-mentioned approaches are yet to achieve a carbon-neutral concrete.

In line with CCUS, metal-organic frameworks (MOF) emerged as an excellent adsorbent material to be employed in capturing CO₂. Yet, despite their attractive characteristics and features, their utilization has been limited to certain applications and is yet to be used by several major industries, including the construction industry. In fact, the incorporation of MOF as a main component in concrete has not been investigated yet. It is hypothesized that the carbon footprint of concrete could be reduced upon the incorporation of MOFs and curing of so-produced concrete using an accelerated carbonation regime.

Concrete masonry units (CMUs) have been widely used in the building industry. They are mass-produced, porous in nature, and made of dry-mix concrete. As a result, CMUs are an ideal candidate for the application of MOF-incorporating concrete and storage of CO₂ through an accelerated carbonation curing process.

1.2 Research Objectives

This research study aims to develop sustainable and eco-friendly concrete that incorporates MOF to capture CO₂ and offset the CO₂ emitted during the manufacture of cement. The specific objectives of this project are as follows:

1. Synthesize and characterize a MOF capable of capturing and storing CO₂ through the accelerated carbonation curing process.
2. Assess the influence of different process parameters on the CO₂ sequestration capacity and performance of MOF-incorporating concrete.
3. Study the effect of incorporating various quantities of MOF on the CO₂ uptake, mechanical properties, and durability of concrete.
4. Evaluate the microstructure characteristics of MOF-incorporating concrete subjected to different curing regimes.

1.3 Relevant Literature

Concrete is the most commonly used construction material worldwide. Its main components include Portland cement, water, and coarse and fine aggregates. In recent years, its global production has rapidly grown. Currently, the concrete production is estimated to be 11 to 13 million m³ (i.e., based on cement content ranging from 350 to 400 kg/m³) and is expected to reach 15 to 17 million m³ by 2050 [1]. Such an excessive need for concrete will have a significant impact on the environment, as the production of cement is responsible for the emission of a considerable amount of greenhouse gases [2, 3].

1.3.1 Background on Portland Cement

Portland cement is the main mineral binding material in concrete that binds the coarse and fine aggregate particles. The process of manufacturing cement is an energy-intensive process and releases excessive amounts of anthropogenic CO₂ [3]. Indeed, its production process undergoes three steps. The first step is the preparation of raw materials, which includes the quarrying, crushing, homogenizing, and grinding of limestone and clay. Using compressed air, drilling, and explosives, the limestone, among other raw materials, is extracted from the quarry and transported to the processing plant using fuel-operating trucks (diesel). Subsequently, the materials are dried, crushed to the optimal size range between 20 and 80 mm, stored in stockpiles, and then transported to the cement plant. Thereafter, they are homogenized and mixed in the silos to decrease the variations in the chemical composition of the raw materials and maintain specific clinker quality. This process is associated with 10% of the total carbon emissions from the production of cement [4, 5].

Furthermore, the second step is the pyro-processing stage. It involves several stages, namely preheating, pre-calcination, calcination, clinker production, and cooling and storage of clinker [6]. In the preheating stage, the raw materials are preheated prior to being added to the main combustion chamber. In the pre-calcination stage, the combustion of fossil fuels, coal, natural gas, and/or petroleum coke is needed to generate the necessary energy to heat the raw materials to approximately 1450°C in the rotary kiln. The energy-related emissions contribute 40% to the total CO₂ emissions from cement production. Subsequently, the raw materials are calcinated within the kiln part, whereby the calcium carbonates in limestone decompose into calcium oxide, leading to the release of CO₂ gas. This stage contributes to about 50% of the cement-related CO₂ emissions. The resultant material at the end of calcination is the clinker, the primary cement component. The produced hot clinker is then stored at a temperature of about 120°C [7].

The third step involves cement preparation. The obtained clinker is ground and blended with gypsum and other additives producing the required cement [6]. The cement is then stored in bags or bulk trucks for transport.

The three-step production of Portland cement releases nearly one ton of CO₂ per ton of cement produced. This accounts for about 7% of the global CO₂ emissions into the atmosphere. The current annual global cement production is 4.5 billion tons, with an estimated increase of approximately 6 billion tons in 2050 [2, 3]. This shows that the cement-induced CO₂ released into the atmosphere is expected to continually increase in the future. Additionally, the manufacturing of cement results in around 2 to 8% of the global power consumption and absorbs almost 12 to 15% of the total industrial energy utilization [8].

1.3.2 Mitigation Techniques of CO₂ Emissions from Cement Production

Over the past 20 years, the cement industry has been confronted by effectively reducing CO₂ emissions to control its detrimental impact on the environment. Researchers have suggested several alternatives to overcome this challenge. The first alternative is the partial and full replacement of cement by pozzolans and supplementary cementitious materials, such as fly ash (FA), silica fume (SF), and ground granulated blast-furnace slag (GGBFS), among others. The second alternative is the substitution of fossil fuels with a lower-carbon content fuel, like sewage sludge. The third alternative is the utilization of

carbon dioxide capture and storage techniques, while the fourth alternative is the use of nanotechnology. The last alternative is the accelerated carbonation of concrete [9].

1.3.2.1 Partial and Full Replacement of Cement by SCMs

Most researchers investigated the blending of cement with pozzolans or SCMs, which originate as by-products or wastes from different industries [10-14]. These materials help improve the performance of concrete either by cementitious or pozzolanic reactions. Replacing an optimum amount of cement with SCMs can lead to an increase in the compressive strength of concrete, a decrease in the cross-sectional area of the structural members, and consequently, a reduction in the overall volume of material required for the structure. Accordingly, lower amounts of CO₂ could be emitted into the atmosphere by the cement industry [15]. Many studies were carried out pertaining to FA and GGBFS substitution for cement in concrete mixes. The results revealed that replacing 25 and 40% of cement with FA and GGBFS in a typical concrete reduced the CO₂ emissions by 14 and 22%, respectively [16, 17]. Further, the effect of replacing 15, 25, 35, and 50% of cement by FA was examined. The authors reported that the 28- and 90-day concrete compressive strengths were the highest in the respective mixes incorporating 15 and 50% FA. The CO₂ released into the atmosphere was decreased by up to 50% [18]. Additionally, substituting ordinary Portland cement (OPC) with 20 and 40% wood fly ash was evaluated. The outcomes showed that incorporating FA in concrete can reduce anthropogenic CO₂ emissions by up to 40% [19]. Also, the effect of using high-volume fly ash (HVFA) in pre-cast concrete was assessed. Half of the cement content was replaced by HVFA. A life cycle assessment (LCA) showed a 25.8% decrease in the released CO₂ emissions into the atmosphere compared to the OPC concrete counterpart [20].

Moreover, it has been reported that using GGBFS as an SCM has a great impact on the greenhouse gas (GHG) emissions associated with cement production. These emissions can be reduced in a range of 22 and 40% [21]. In fact, replacing cement with 80% blast furnace slag resulted in a drop of 66% in the emitted CO₂ emissions [22]. A study has examined the effect of incorporating various replacement ratios of slag waste in high early strength concrete. The results showed that using 30% slag as SCM has curbed the CO₂ emissions by 30% while reducing the strength by 11% [23].

On the other hand, several investigations demonstrated the use of SCMs, typically FA and GGBFS, as a total replacement of ordinary Portland cement (OPC) to produce inorganic geopolymer concrete (GPC). The impact of mixture components on the fresh and hardened concrete properties has been investigated. Several studies showed that the use of FA/GGBFS blended geopolymer composite was a suitable alternative to a cement-based composite from workability, setting time, and compressive strength standpoints [24]. The performance of FA/GGBFS blended geopolymer concrete was superior to that of counterparts made with only a single binder, i.e., FA or GGBFS. Indeed, to obtain similar design compressive strength, less binder was needed in binary mixes than in single binder mixes [25, 26]. Furthermore, the combination of FA and GGBFS could eliminate the need for heat curing that is typically needed in FA-based geopolymers. Meanwhile, the performance of GGBFS-based and blended geopolymers was improved upon utilizing a combined curing regime of air and water rather than air or water curing individually [27-29]. Its microstructure characteristics were typical of calcium aluminosilicate hydrate (C-A-S-H) gel with some traces of hydrotalcite and calcium silicate hydrate (C-S-H) gel [30, 31]. However, while the use of such a blended cement-free binder was not as effective in producing lightweight geopolymer concrete [32], the bond capacity of FA/GGBFS blended mortar was comparable to that of cement-based mortars in carbon fabric-reinforced matrix composites [33]. Other industrial waste materials have also been utilized, including ladle slag, metakaolin, and bauxite residue, among others [34-37].

The utilization of GPC in the construction industry has ensured the reduction of CO₂ footprint by up to 80% compared to OPC concrete, owing to the lower carbon footprint of such SCMs compared to OPC [38]. One study showed that the quantified CO₂ emissions of fly ash-based GPC were 63% lower than that of OPC concrete of the same compressive strength [39]. Other work investigated the effect of metakaolin-based geopolymer (MKG) on GHG emissions. Comparing the results to blended OPC mixes, MKG had reduced the anthropogenic carbon dioxide by 27-45% [40]. Additional research reported that the CO₂ emissions released from the geopolymer concrete were about 9% less than the OPC concrete [41]. Furthermore, geopolymer and alkali-activated binary concrete mixes could significantly curb GHG emissions by up to 64 and 45% compared to the OPC concrete [42, 43].

1.3.2.2 Substitution of Fossil Fuels by a Lower-Carbon Content Fuel

The substitution of fossil fuels with alternative fuels can substantially reduce the CO₂ emissions incurred by the manufacture of cement. The amount of released CO₂ is affected by the type of fuel used (i.e., coal, fuel oil, natural gas, and alternative fuels) [44]. Animal fat, rubber, used chemicals, impregnated sawdust, sewage/industrial sludge, and paper sludge were utilized as alternative fuels to be co-combusted in cement kilns. The fuel substitutions could ideally range from 80% to 100% [45]. More realistically, the values have not exceeded 70%. As a result, the carbon emissions associated with cement manufacturing could be reduced by up to 30%. However, this is yet to be achieved [46].

A study has investigated and introduced spent carbon lining, used industrial lubricants, and used tires in a step to reduce CO₂ emissions. It has been proven that the used industrial lubricants were the most suitable alternative fuel to replace coal. While the energy content was the highest, the overall produced CO₂ emissions were the lowest [47]. Another study examined the utilization of meat and bone meal (MBM), municipal solid waste (MSW), plastic waste, tire, and sugarcane bagasse as a secondary fuel in manufacturing cement. The authors reported that apart from the sugarcane bagasse, the tested alternative fuels were capable of reducing CO₂ emissions and the thermal energy requirement compared to that of coal. The highest reduction of up to 30% of the total thermal energy requirement was achieved by replacing coal with MBM. The anthropogenic CO₂ emissions and the thermal energy requirement were decreased by 4.7 and 6.4% [48].

Additionally, the effect of using 70 alternative fuels known as “solid secondary fuel”, such as textiles, plastics, tires, papers, and rubber, on the CO₂ emissions was evaluated. The results revealed that the amount of CO₂ emitted from the co-combustion of coal with 70% alternative fuel was reduced by 25% [49]. On the other hand, one research that focused on the usage of sewage sludge as a secondary fuel in manufacturing cement reported a reduction in carbon emissions of about 10% [46].

Moreover, the use of non-recycled plastics and paper residue (NRPP), known as “engineered fuel” (EF), as an alternative fuel in the cement industry was studied. Research outcomes indicated that the use of one ton of NRPP in place of coal resulted in a reduction of approximately three tons of CO₂ emissions to the atmosphere. The emissions dropped

from 390 kg to 137 kg CO₂ per ton of clinker as coal content reduced from 100 to 25%, respectively [50]. In another work, the utilization of wood-derived fuel (WDF) as alternative biomass fuel in the co-combustion process of cement production was assessed. The life cycle assessment (LCA) results showed that the co-combustion of 20% WDF with coal was capable of lowering anthropogenic CO₂ emissions by about 16% while decreasing upstream energy consumption by around 14% [51]. Moreover, an investigation evaluated the usage of processed material recovery facilities (MRFs) in solid recovered fuel (SRF) in the manufacturing of cement. The results indicated that the utilization of SRF as an alternative fuel could offset the release of CO₂ emissions by at least 1.4% compared to the reference case, i.e., coal was used as a fuel source [52].

1.3.2.3 Carbon Dioxide Capture, Utilization, and Storage

Carbon dioxide capture, utilization, and storage have been highlighted as one of the most cost-effective ways to curb CO₂ emissions associated with global industries, including the cement industry. Different techniques have been investigated and developed for the capture of CO₂ at the point of combustion, including post-combustion, pre-combustion, and oxy-fuel combustion capture [45]. In the post-combustion technique, the CO₂ is separated at low pressure from the flue gas that is generated by burning fossil fuels in the air. Then, it is captured and stored in a reservoir while the rest of the exhaust gas is discharged into the atmosphere. The efficiency of this method increases as the CO₂ concentration increases in the flue gas. Conversely, in the pre-combustion process, the CO₂ is removed from fossil fuels before the completion of the combustion. The gas is exposed to either steam or oxygen to react and form a “synthesis gas” comprising a combination of hydrogen and carbon monoxide. The latter product then reacts with steam to produce hydrogen and carbon dioxide that are separated using a chemical or physical absorption process, captured, and stored. Furthermore, in the oxy-fuel combustion capture technique, the fuel gas is burnt using pure oxygen rather than air. The generated flue gas contains high concentrations of CO₂ and water vapor. The CO₂ is captured by lowering the temperature of the flue gas in multiple heat exchangers to condense the water vapor and separate CO₂ [45, 53].

In 2003, it was reported that using the carbon capture technique in the cement industry may reduce carbon dioxide emissions by 65-70% [45]. Nevertheless, a 57% drop

in carbon emissions could be attained by 2030 through CCUS based on three emission scenarios established in the cement production facilities in China. In addition, the outcomes of one research work highlighted a potential reduction in the cost of capturing CO₂ from cement production ranging between 5 and 20% compared to coal-fired power generation [54]. Similar results were reported in a study commissioned by the International Energy Agency Greenhouse Gas Research and Development Programme (IEAGHG). In this work, the environmental impact of cement produced in newly-build cement plants while employing post-combustion and oxy-combustion CO₂ capture was analyzed from the perspective of lifecycle assessment [55]. The results demonstrated that the overall reduction in CO₂ emissions from the oxy-combustion CO₂ capture method was 52%, while it reached 77% from post-combustion CO₂ capture technology [56].

1.3.2.4 Nanotechnology

Past research focused on the utilization of nanotechnology to mitigate CO₂ emissions released from the cement industry. In one work, the addition of 1% zinc oxide nano-powder into a cement mix reduced the CO₂ gas emissions and energy consumption, owing to the drop in clinker production temperature from 1450°C to 1300°C [57]. Another research studied the effect of substituting cement in a mortar with nano calcium carbonate particles obtained from CO₂ in a flue gas generated during cement production. The outcomes pointed out the possibility of reducing the carbon footprint of cement in construction by decreasing the cement content in the mortar mix [58]. Moreover, a study investigated the effect of adding nano-TiO₂ on the CO₂ sequestration of cement paste subjected to accelerated carbonation curing. Compared to the reference paste, the addition of 0.5, 1, and 2% TiO₂ nanoparticles increased the CO₂ uptake by 18.5%, 20.5% and 38.4%, respectively [59].

1.3.2.5 Accelerated Carbonation of Concrete

Accelerated carbonation of concrete is a process of exposing concrete at an early age to CO₂ gas under controlled conditions. It involves a chemical reaction between CO₂ and main silicate phases in cement, including tricalcium silicate and dicalcium silicate, in the presence of water, to produce calcium silicate hydrate (C-S-H) and calcium carbonate (CaCO₃). It can also take place in hardened concrete at a later age, where CO₂ reacts with

hydration products, such as calcium hydroxide (CH) and C-S-H, forming CaCO_3 and silica gel [60]. Many factors influence the accelerated carbonation process, such as CO_2 concentration and pressure, preconditioning conditions, mixture proportions (i.e., sand-to-cement ratio), and type of cementitious material [61]. Accelerated carbonation of concrete showed a promising capacity to reduce the cement-induced carbon footprint. Owing to its ability to sequester CO_2 and improve the mechanical and durability properties of mortars and concrete, it has been employed in curing various concrete products [62]. Depending on the carbonation methodology applied, carbon uptake of lightweight OPC concrete masonry units (CMUs) could reach up to 35%, by cement mass. However, within a 24-hour time frame, the uptake reached 24%, by cement mass [63]. Other work employed Portland limestone cement (PLC) as a binder in CMUs. The findings revealed that after 18-hour initial curing and 4-hour carbonation curing, the CO_2 uptake of PLC concrete reached 18%, by cement mass [64]. Reaction products were mainly calcium silicate hydrate (C-S-H) gel and calcium carbonate in its different polymorphs, i.e., calcite, aragonite, and vaterite [65]. In a different approach, the carbon uptake of lightweight concrete reached 13 and 20% in 4- and 18-hour pseudo-dynamic carbonation, respectively [66].

Other work studied the effect of replacing cement with different percentages of biochar on the carbonation degree, hence the CO_2 sequestration. The experimental results revealed that the accelerated carbonation curing of the biochar-blended specimens at 5% CO_2 concentration and 0.1 MPa pressure resulted in a higher degree of carbonation. It reached 89% at 28-day age compared to the plain mortar that exhibited 39% carbonation [67]. Another research has developed an alternative binary binding system for engineered cementitious composite (ECC). Magnesium oxide (MgO) and fly ash were used as binders. Under the accelerated carbonation curing at 99.8% pure CO_2 , the 24-hour carbonated reactive MgO-based ECC (with 50% MgO) lowered the net CO_2 emissions by about 65% compared to the conventional ECC [68].

Furthermore, the effectiveness of implementing accelerated carbonation curing to concrete with partial substitution of cement by supplementary cementitious material (SCMs) to curb CO_2 emissions associated with cement production was analyzed. Several studies were carried out pertaining to fly ash (FA) replacement of cement in concrete

mixes exposed to accelerated carbonation. Research findings showed that the carbonation curing of concrete incorporating 20 and 50% FA for 2, 12, and 24 hours at 99.8% CO₂ concentration and 5-bar pressure led to higher CO₂ sequestration [69]. Another study was conducted using class II fly ash as an SCM with a replacement percentage of 20%, by cement weight. Initial curing was completed for 24 h at 20±3°C, and then carbonation curing was applied for 4 hours at 20% CO₂ concentration, 20±3°C, and 60±5% RH. The results demonstrated that the mix incorporating 20% FA possessed the highest strengths and the highest CO₂ sequestration capacity of 13.94%, by mass of the initial binder. On the other hand, it exhibited the largest decrease in the permeability, most reduction in the total porosity, and superior densification of the microstructure [70].

Other work highlighted the use of argon-oxygen decarburization (AOD) slag as an SCM in concrete exposed to carbonation curing. In this research, cement was replaced by percentages of 0, 30, and 60%, by weight. Carbonation curing was performed for 14 days at 60% RH and different CO₂ concentrations and temperatures. The results revealed that the increase in the CO₂ concentration and substitution level of AOD slag, regardless of the curing temperature, resulted in an increase in the CO₂ uptake of the incorporated mixes [71]. An additional study indicated that the carbon uptake in the Ultra-High Performance Concrete (UHPC) using fresh state carbon curing was the highest for the mix, replacing 30% of cement by GGBFS. Up to 80 kg of CO₂ could be sequestered per cubic meter of UHPC at 3 bar pressure and 16 hours of carbonation [72].

An investigation analyzed the effectiveness of implementing accelerated carbonation to concrete by partially replacing cement with magnesia (MgO). Research findings showed that the carbonation curing at a 99.9% atmospheric CO₂ concentration, 23±2°C, and 98% RH for 7, 28, and 56 days preceded by initial curing for 24±2 h at 23±2°C and 90% RH resulted in a carbon uptake of up to 25.2%, by sample weight, for the mix containing 10% MgO. Reaction products, mainly magnesium calcite (MgCO₃) and nesquehonite (MgCO₃·3H₂O), densified the microstructure and led to higher microhardness compared to the cement pastes [73].

In other work, cement was replaced with 10% limestone filler. Cement pastes were preconditioned at 65% RH and then carbonation-cured at a pressure of 6 bars and RH of 65% for 28 days. Results indicated that accelerated carbonation curing led to a reduction

in the porosity and water permeability and caused an increase in the CO₂ uptake capacity. Such findings were attributed to the formation of carbonation products on the limestone particles, which served as nucleation sites for calcite precipitation [74].

Furthermore, the impact of the accelerated carbonation on concrete incorporating volcanic ash (VA) as an SCM was examined. Portland cement was replaced by various ratios of VA (0, 20, 30, 40, and 50%, by mass of cement). After 24-hour initial curing and 28-day carbonation curing at a 5% CO₂ concentration, 25°C, and 60% RH, the carbonated VA-cement blended pastes exhibited a linear increase in the carbon uptake capacity with the VA replacement. The maximum CO₂ sequestration was 30.7%, by binder mass [75].

Moreover, self-ignited coal gangue (CG) was utilized as an SCM in carbonation-cured concrete. Replacement percentages of 10, 20, 30, and 50% were used. The initial curing was carried out for 24 hours at 20±3°C, while the carbonation curing was conducted for 2 to 4 hours at a 20% CO₂ concentration, 20±3°C, and 60±5% RH, followed by subsequent hydration. The results indicated that the highest CO₂ uptake was 11.46%, by binder mass, for the carbonated mix blended with 20% CG [76].

The effect of incorporating waste autoclaved aerated concrete (WAAC) powder in concrete exposed to carbonation curing was assessed. WAAC replaced cement by 10, 20, 30, and 50%, by binder mass. The conditioning entailed initial curing for 24 hours at 20±3°C, carbonation curing for 2 to 4 hours at a 20% CO₂ concentration, 20±3°C, and 60±5% RH, and subsequent hydration at 22±3°C and 90% RH. The findings revealed that the process increased the CO₂ uptake, by binder mass, from 11.23% for cement-based mixes to 19.02% for those incorporating up to 50% WAAC [77].

Several studies were conducted to examine the effect of cement replacement with blends of SCMs on the properties of carbonation-cured pastes and concrete. Pastes were made with 40% GGBFS and 0 to 40% reactive MgO as cement replacement. Initial curing was performed for 24±2 hours at 23±2°C and 98% RH, followed by carbonation curing for 7, 28, and 56 days at a 99.9% CO₂ concentration, 23±2°C, and 98% RH. Results showed that the total CO₂ sequestration was the highest and the lowest for the mixes containing 20% and 40% MgO, correspondingly [78]. In another work, the effect of carbonation curing on ternary blends made with Portland cement and a combination of metakaolin and limestone powder (weight ratio of 2:1) with replacement percentages of 0,

15, 30, and 45%, by mass, was examined. Pre-curing for 24 hours at 20°C, CO₂ curing for 0.5, 13, and 27 days, and sealed curing for 28 days at 20°C were performed. The carbonation rate and CO₂ uptake increased with higher replacement of PC and longer duration of carbonation curing. Yet, this was associated with a reduction in the compressive strength and an increase in the volume of permeable voids and sorptivity coefficient [79].

1.3.3 Metal-Organic Frameworks

In the past two decades, metal-organic frameworks (MOF) have emerged as a new class of crystalline porous material and excellent adsorbent material for capturing different gases [80]. They are synthesized using metal-based nodes (single ions or clusters) bridged by organic linking groups to form a one-, two-, or three-dimensional coordination network [81]. Compared to traditional adsorbent materials used in the industry, MOFs provide superior characteristics, including but not limited to the higher surface area, high crystallinity with well-defined pore properties, easily tunable, adaptable structures, and adjustable chemical functionality [82]. These attractive features promote their use in many industrial applications, such as gas storage, luminescence, catalysis, nanoparticle precursor, electrochemistry, and as a sensor in technology [83].

Several past studies have reported the use of the MOFs in storing different gases, especially CO₂, as a means of reducing their atmospheric concentration. MOFs with high CO₂-capturing capacity are expected to exhibit high selectivity of CO₂ gas over other gases. Several MOF-based materials have been developed for CO₂ capture. For instance, MOF-5 and Mg-MOF-74 have uptakes of 1.1 and 8.0 mmol.g⁻¹, respectively. Conversely, HKUST-1 demonstrated a carbon capture potential of 3.3 mmol.g⁻¹, while UiO-66 had a carbon capture capacity of 2.3 mmol.g⁻¹. Additionally, the CO₂ uptake of ZIF-20 and PCN-5 were 70 mL.g⁻¹ and 210 mg.g⁻¹, respectively [84].

Three primary technologies have been utilized for capturing CO₂ using MOFs, namely pre-combustion, post-combustion, and oxy-fuel combustion [85]. The selection of the technology is mainly based on its CO₂ feed input conditions, advantages, and disadvantages [86]. Past research focused on the addition of different MOFs to the pre-combustion process. Research findings showed that MOFs improved the separation of CO₂ from the CO₂/H₂ mixture. They exhibited better performance than zeolites, owing to their

higher porosities, which led to higher CO₂ uptake [87]. Other studies investigated the efficiency of MOFs in the CO₂ capture under post-combustion conditions. A variety of MOFs was used, including ZIF-8, HKUST-1, and MIL-53 (Al). The results showed a remarkable increase in the CO₂ uptake capacity [88]. Besides, they reported higher CO₂/H₂ and CO₂/N₂ selectivity compared to that of other nano-porous adsorbents [89]. Nevertheless, the authors highlighted that the application of MOFs in the oxy-fuel combustion process was restricted within the carbon capture processes. This was because the produced flue gas, in this method, was enriched with CO₂ and water vapor [90]. As a result, the purification was achieved through the condensation of water vapor; thus, the capture of CO₂ was not required [91].

Based on these CO₂-capture results, the use of MOFs as a main component in concrete production could alleviate the environmental impact of CO₂ emissions associated with the manufacture of cement. Yet, MOFs have not been used in concrete mixes for the purpose of CO₂ capture.

1.4 Outline and Organization of Thesis

The thesis structure is organized and divided into the following five chapters:

- Chapter 1: A brief summary of the problem statement is provided, accompanied by the proposed research objectives. Subsequently, a literature review on Portland cement and mitigation techniques of CO₂ emissions from the production of cement and MOF is given. Lastly, the outline and organization of the thesis and research significance are highlighted.
- Chapter 2: A detailed description of the test program is given. The properties of the used materials and experimental methodology are furnished.
- Chapter 3: The experimental test results, comprising the CO₂ uptake, phenolphthalein evaluation, compressive strength, water absorption, and permeable pore voids volume of the carbonated MOF-incorporating concrete mixes, are presented.
- Chapter 4: The microstructure evaluation of the carbonated MOF-incorporating concrete mixes is stated in this chapter, including powder X-ray diffraction analysis

(PXRD), scanning electron microscope (SEM), and Fourier transform infrared (FTIR) spectroscopy.

- Chapter 5: Main conclusions and outcomes, limitations of the work, and recommendations for future studies on the use of MOF in concrete are listed.

1.5 Research Significance

The ever-increasing level of CO₂ emissions to the atmosphere is a pressing contemporary environmental and ecological concern. The construction industry is responsible for a significant amount of these anthropogenic emissions through the production of concrete and its binder component, cement. Extensive research has been carried out to alleviate these cement-induced anthropogenic CO₂ emissions, with scientists and environmentalists suggesting various mitigation techniques, such as the substitution of fossil fuels with a lower carbon content fuel, CCUS, partial and full replacement of cement, and accelerated carbonation curing. In line with CCUS, MOFs have emerged as excellent adsorbent materials to be employed in CO₂ capture. Nonetheless, despite their attractive characteristics and features, their utilization has been limited to certain applications and is yet to be used by several major industries, including the construction industry. In fact, the incorporation of MOFs as a main component in concrete has not been investigated yet.

This thesis aims to develop sustainable and eco-friendly concrete that incorporates MOF to capture CO₂ and offset the carbon footprint associated with the manufacture of cement. MOF-incorporating concrete will be subjected to an accelerated carbonation process by exposing it to concentrated CO₂ gas in a carbonation chamber for various durations, under different pressures, and after diverse initial curing regimes. The carbon uptake capacity, mechanical properties, durability, and microstructure of the MOF-incorporating concrete will be evaluated. Carbonation curing of the MOF-incorporating concrete serves to permanently sequester CO₂ and improve the mechanical and durability properties.

Chapter 2: Experimental Program

2.1 Overview

This chapter sheds light on the detailed experimental program carried out in this research study. The properties of the materials used in this work, including cement, aggregates, and water, were reported. Subsequently, the procedure for synthesizing and activating the MOF was described. The characteristics of the produced MOF are presented. Furthermore, the concrete mixture proportions, sample preparation, and curing regimes are mentioned. Lastly, the methodology for evaluating the carbon uptake, performance, and microstructure of concrete was furnished.

2.2 Test Program

Various parameters play a critical role in the accelerated carbonation curing process of concrete, including the initial air curing duration, accelerated carbonation curing duration, CO₂ pressure inside the chamber, and quantity of MOF incorporated into the concrete mix. The initial air curing duration was selected to be either 4 or 20 hours. Based on a previous study, initial air curing durations of less than 4 hours did not remove a sufficient amount of water from the concrete to allow for CO₂ percolation. As a result, the CO₂ uptake was limited. Meanwhile, extending it beyond 20 hours led to very short carbonation curing durations, given that the total curing duration should be limited to 24 hours to maintain industrial feasibility and consequently low CO₂ uptake [63]. Furthermore, the accelerated carbonation curing duration was chosen to be 4 and 20 hours to investigate the effect of short and long carbonation periods on the CO₂ uptake and performance of concrete within a 24-hour time frame. The carbonation curing process was preliminarily conducted at a pressure of 1, 2, and 5 bars. The results obtained from 1 and 2 bars were comparable, so the lower pressure of 1 bar was selected. Moreover, the higher pressure of 5 bars was tested to investigate its effect on the CO₂ uptake and performance of MOF-incorporating concrete. A previous study showed that carbonating concrete at 5 bars pressure resulted in maximum CO₂ uptake [92]. The experimental test matrix is presented in Table 1. To study the effect of each parameter, a total of 11 concrete mixes were designed and cast. For each group, at least two mixes were prepared: one mix was kept as a control or benchmark, i.e., carbonated mix without the addition of MOF, while

the remaining carbonated mix(es) incorporated the MOF. The role of the control was to compare carbonated MOF-incorporating concrete mixes to counterparts that did not include MOF. Mixes were designated as Xa-Yc-ZP-WM, where X represented the initial air curing duration in hours, Y denoted the accelerated carbonation curing duration in hours, Z described the carbonation pressure inside the chamber in bars, and W represented the quantity of MOF incorporated into the mix as a percentage of binder mass. For instance, mix M1-3 (20a+4c-1P-9M) entails a mix made with 9% MOF, by cement mass, that is subjected to 20 hours of initial curing and 4 hours of carbonation curing at a pressure of 1 bar.

Table 1: Experimental test matrix

Group	Mix ID	Mix designation	Initial curing duration (h)		Accelerated carbonation duration (h)		CO ₂ pressure (bar)		Quantity of MOF (%)			
			4	20	4	20	1	5	0	3	6	9
Control	C0	0a+0c-0P-0M							x			
A	C1	20a+4c-1P-0M		x	x		x		x			
	M1-1	20a+4c-1P-3M		x	x		x			x		
	M1-2	20a+4c-1P-6M		x	x		x				x	
	M1-3	20a+4c-1P-9M		x	x		x					x
B	C2	4a+4c-1P-0M	x		x		x		x			
	M2	4a+4c-1P-6M	x		x		x				x	
C	C3	20a+20c-1P-0M		x		x	x		x			
	M3	20a+20c-1P-6M		x		x	x				x	
D	C4	20a+4c-5P-0M		x	x			x	x			
	M4	20a+4c-5P-6M		x	x			x			x	

The mixes were divided into five groups. The first group, denoted as control (0a+0c-0P-0M), was a non-carbonated concrete mix. It was placed in a sealed plastic bag after demolding without initial curing, carbonation curing, or MOF and served as a benchmark. The groups are listed as follows:

- Group A aimed to examine the effect of MOF quantity. It included four concrete mixes subjected to 20 hours of air curing followed by 4 hours of carbonation. One mix had no MOF, while the other three had 3, 6, and 9% MOF addition by binder mass.

- Group B was formulated to study the effect of shorter initial curing duration and 4-hour carbonation curing. While one mix did not include MOF, the other had 6% MOF, by binder mass, as the results showed that exceeding 6% MOF content did not improve carbon uptake or performance.
- Group C included two mixes (i.e., one with MOF and one without) to evaluate the influence of prolonged initial curing and carbonation curing durations (20 hours each).
- Group D was created to examine the impact of carbonating concrete at a higher pressure of 5 bars. One mix incorporated 6% MOF while the other had no MOF.

2.3 Materials

ASTM Type I ordinary Portland cement (OPC) was used as the binder in the concrete mixes [93]. It was locally sourced from the Emirates Cement factory. The chemical composition of the OPC is illustrated in Table 2, while its scanning electron microscope (SEM) micrograph is presented in Figure 1.

Table 2: Chemical composition of cement

Oxide compound	SiO ₂	CaO	Al ₂ O ₃	Fe ₂ O ₃	MgO	NaO	SO ₃
Weight (%)	19.9	63.2	4.9	2.3	2.5	0.8	3.8

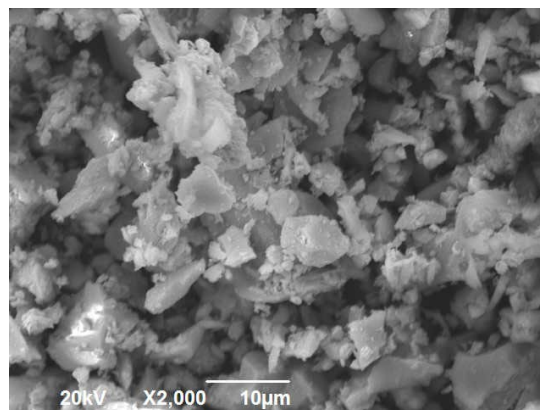


Figure 1: SEM micrograph of OPC

Crushed dolomitic limestone aggregates, sourced from Ras Al Khaimah, were utilized in the concrete mixes. Their sieve analysis, presented in Figure 2, was within the upper and lower bounds specified by ASTM C33 [94]. It shows that the maximum size of the aggregates exceeded 4.75 mm. As such, the aggregates used herein could be considered a combination of coarse and fine aggregates. Their physical properties are summarized in Table 3. Furthermore, Figure 3 illustrates the FTIR spectrum of the aggregates. The strong and sharp absorption bands at 1430, 877, and 725 cm^{-1} were assigned to the carbonate (CO_3^{2-}) bending vibration in calcite. Moreover, tap water with a pH of 7.1 was the mixing water used in the concrete mix. It satisfied the requirements of ASTM C1602 [95].

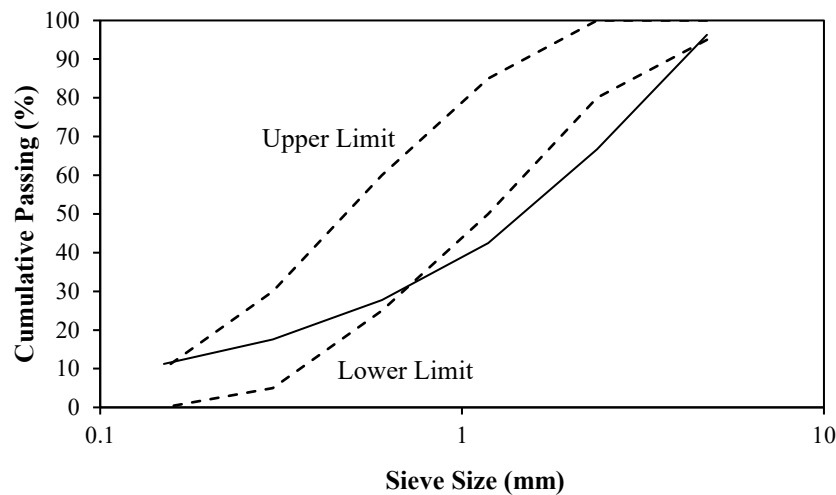


Figure 2: Sieve analysis of crushed limestone aggregates

Table 3: Physical properties of crushed limestone aggregates

Property	Unit	Standard test	Aggregates
Maximum size	mm	ASTM C136 [96]	5
Dry-rodded density	kg/m^3	ASTM C29 [97]	1635
Absorption	%	ASTM C127 [98]	6.05
Surface area	cm^2/g	ASTM C136 [96]	77.38
Specific gravity	-	ASTM C127 [98]	2.80
Fineness modulus	-	ASTM C136 [96]	3.07

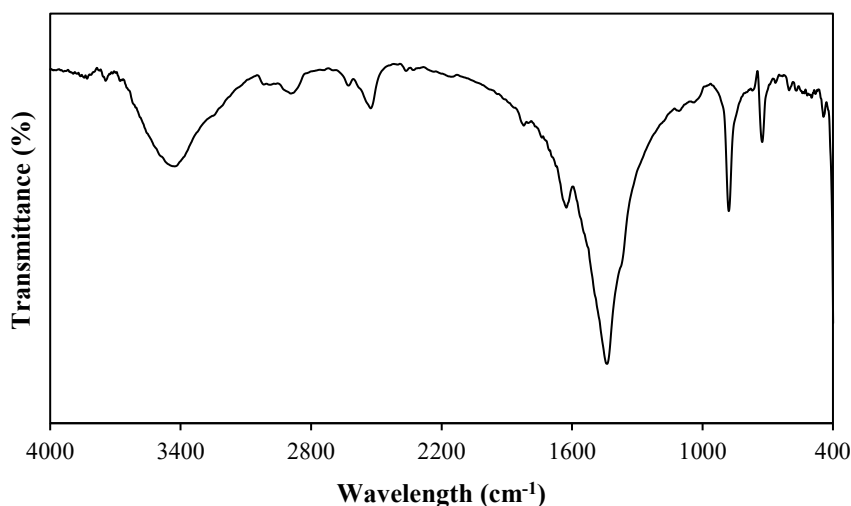


Figure 3: FTIR spectra of crushed limestone aggregates

NH₂-MIL-125 was selected as a CO₂ adsorbent to be incorporated into the concrete mixes. Its remarkable features, including high CO₂ adsorption capacity (136 mg/g) and high Brunauer, Emmett, and Teller (BET) surface area of 1530 m²/g, made it an ideal candidate for capturing CO₂ through accelerated carbonation curing [99]. The MOF was prepared and synthesized in the chemistry lab, as explained in detail in the following section. Its density was found to be 0.35 g/cm³. It was characterized by PXRD, SEM, and FTIR, as shown in Figures 4, 5, and 6, respectively. The PXRD pattern indicated well-defined diffraction peaks of 6.8°, 9.7°, 11.6°, 16.5°, and 18.1°, which were indexed as the diffractions of (011), (002), (121), (222) and (132) crystalline planes of NH₂-MIL-125. The morphology of the MOF, as displayed in the SEM image (Figure 5), was thin and disk-like in shape with an average particle size of 1 μm. However, the FTIR spectrum (Figure 6) demonstrated that the strong and wide absorption band at 3440 cm⁻¹ was assigned to the stretching vibrations of the primary amines (-NH₂ group) of the organic linker. The peaks located at 1625 and 1544 cm⁻¹ were attributed to the bending vibrations of N-H moiety and asymmetric stretching vibration of the carbonyl group, respectively. Furthermore, the various bands in the region of 1400-1700 cm⁻¹ were attributed to the -COOH group. The absorption bands at approximately 1380 and 1252 were assigned to the terephthalate and aromatic C-N moieties, correspondingly. The O-Ti-O vibrations were obtained in the region of 400-800 cm⁻¹. These results of the characterization

techniques were in accordance with several past works concerning the synthesis of NH₂-MIL-125 [99-101].

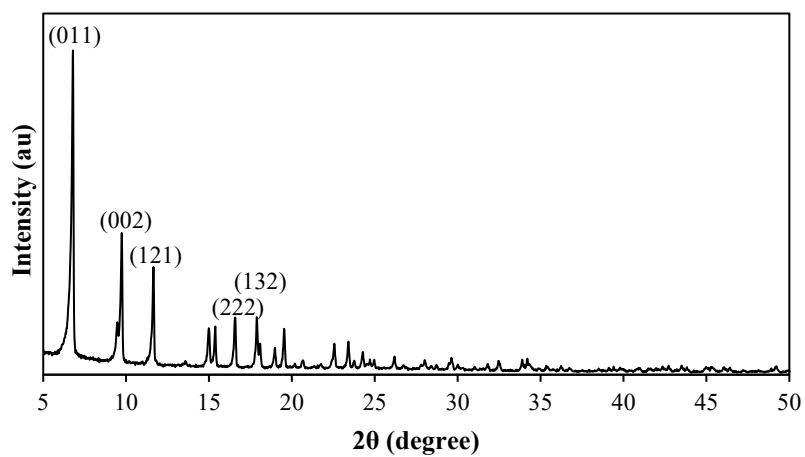


Figure 4: PXRD pattern of NH₂-MIL-125 (Ti)

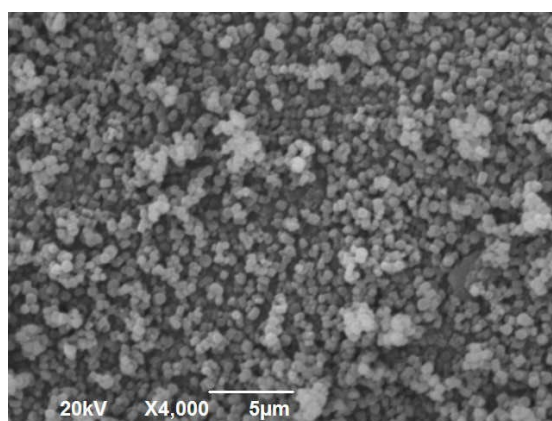


Figure 5: SEM micrograph of NH₂-MIL-125 (Ti)

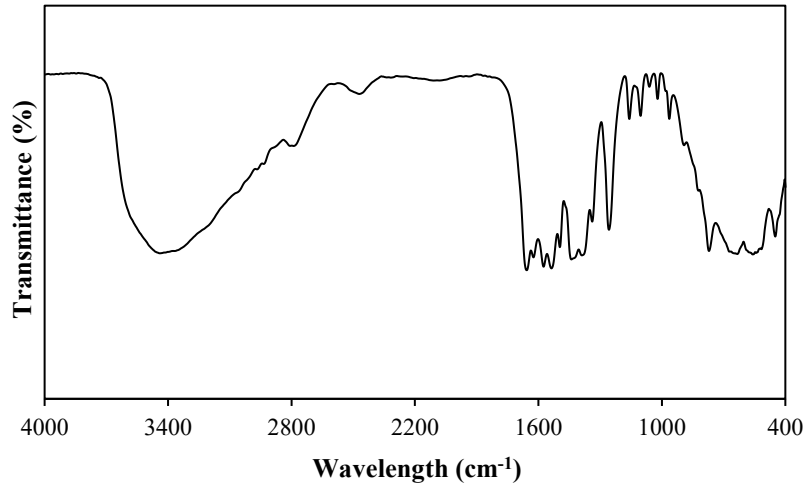


Figure 6: FTIR spectrum of MOF, NH₂-MIL-125 (Ti)

2.4 Methodology

The experimental investigation aimed to assess the carbon uptake, properties, and microstructure of the cast concrete mixes. The MOF synthesis and activation, concrete mix proportions, concrete sample preparation, curing regimes, carbon uptake, phenolphthalein carbonation indicator, concrete performance evaluation, and microstructure characterization are described in the following subsections.

2.4.1 Metal-Organic Frameworks (MOFs) Synthesis and Activation

The MOF, NH₂-MIL-125 (Ti), consisted of a repeating unit cell. Each unit cell was composed of six ligands (linkers) and a metal cluster. Titanium isopropoxide, 97% (C₁₂H₂₈O₄Ti) and 2-Aminoterephthalic acid, 99% (C₈H₇NO₄) were used to represent the metal ions (cluster) and the linkers, respectively.

As the selected MOF, NH₂-MIL-125 (Ti), was not commercially available in large quantities, it was synthesized on a lab scale in the Chemistry Department laboratory at the United Arab Emirates University. The MOF was synthesized by dissolving the 2-Aminoterephthalic acid in a mixed solvent of N, N-Dimethylformamide, 99% (DMF), and methanol by magnetic stirring in a pressure vessel under heating in an oil bath. Then, the titanium isopropoxide was added, and the mixture was stirred for 24 hours while heating at 150°C, as illustrated in Figure 7. After cooling to room temperature, the solid yellow powder was filtered and washed twice with dichloromethane (DCM) and thrice with

methanol (Figure 8). Finally, NH₂-MIL-125 (Ti) was activated by heating at 200°C for 6 hours under a vacuum to remove any trapped solvent molecules, as displayed in Figure 9. At the end of each synthesis process, a sample of MOF was examined for phase purity using PXRD and compared to that previously reported in the literature [99]. The total synthesis process to produce 25 g of MOF required a duration of up to 48 hours.



Figure 7: NH₂-MIL-125 (Ti) synthesis



Figure 8: NH₂-MIL-125 (Ti) filtration and washing



Figure 9: NH₂-MIL-125 (Ti) activation

2.4.2 Concrete Mix Proportions

Three trial mixes were designed and cast, as illustrated in Figure 10. The mix proportions of each mix are shown in Table 4. T1, T2, and T3 were designed to have a cement-to-aggregate ratio of 0.25, 0.20, and 0.17, respectively. All mixes had a water-to-cement ratio of 0.45. To select the most appropriate mix for accelerated carbonation curing, the compressive strength and permeable pore voids volume tests were conducted. The results, presented in Table 5, show that mixes T1 and T2 have similar 1, 7, and 28-day strengths and comparable permeable pore voids volume. However, mix T3 has 3 and 1% lower 28-day compressive strength than T1 and T2, respectively, but 15 and 8% higher permeable pore voids volume. With a limited loss in strength and a substantially higher void volume, mix T3 was selected for further analysis, as it will have higher diffusivity of CO₂ and will therefore achieve better carbon sequestration potential.



Figure 10: Trial control mixes

Table 4: Mix proportions of trial concrete mixes

Mix designation	Cement (kg/m³)	Aggregates (kg/m³)	Water (kg/m³)
T1	445	1785	200
T2	380	1900	171
T3	340	2040	153

Table 5: Trial control mixes properties

Mix designation	1-day f'_c (MPa)	7-day f'_c (MPa)	28-day f'_c (MPa)	Permeable pore voids volume (%)
T1	25.3 ± 1.6	32.5 ± 0.6	33.0 ± 0.7	14.3 ± 0.1
T2	25.6 ± 1.8	32.0 ± 1.1	32.5 ± 0.7	15.3 ± 0.3
T3	13.8 ± 1.3	31.7 ± 1.3	32.1 ± 0.8	16.5 ± 0.6

2.4.3 Concrete Sample Preparation

The concrete samples were prepared by thoroughly mixing cement, fine aggregates, and coarse aggregates for three minutes under an ambient temperature of $25 \pm 2^\circ\text{C}$ and RH of $50 \pm 5\%$ using a concrete mixer. The water was then gradually added to the dry components and further mixed for two minutes. Subsequently, the MOF (if any) was homogeneously incorporated into the mix by mixing for another two minutes to ensure uniformity. The fresh concrete was cast and placed into 50 mm x 50 mm x 50 mm cubic molds in two layers. Each layer was vibrated on a vibrating table for about 10 seconds to ensure proper consolidation, in accordance with ASTM C192 [102]. The specimens were directly demolded after casting to reduce the free water content through evaporation and, consequently, allow for adequate CO_2 diffusion into the sample. Indeed, past research has highlighted that excess free water may hinder the diffusion of CO_2 , while the lack of free water could prevent the dissolution of CO_2 from reacting with calcium-carrying compounds in cement [63]. Also, it is worth noting that demolding was possible at a very fresh state because the cast concrete was a dry mix, similar to that used in concrete masonry units (CMUs). Concrete mixes after casting and curing are shown in Figure 11.



Figure 11: Concrete mixes after casting and curing

2.4.4 Curing Regimes

After demolding, fresh concrete samples were cured. Curing was divided into three categories, namely pre-carbonation curing (i.e., initial curing), accelerated carbonation curing, and post-carbonation curing (i.e., subsequent hydration).

2.4.4.1 Pre-Carbonation Curing

In the pre-carbonation (initial) curing scheme, the specimens were subjected to open-air curing, as demonstrated in Figure 12. The samples were air-cured in the laboratory at ambient conditions of $50\pm 5\%$ RH and a temperature of $25\pm 2^\circ\text{C}$ until testing age.

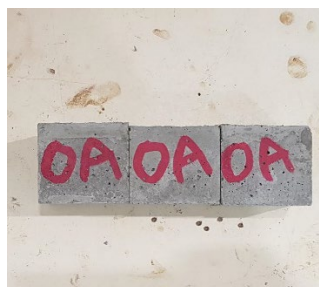


Figure 12: Open-air curing of concrete samples

2.4.4.2 Accelerated Carbonation Curing

The accelerated carbonation curing was performed in a manufactured sealable carbonation chamber equipped with a safety valve. The chamber was attached to a CO_2 cylinder with a purity of 99.5%, as displayed in Figure 13. The pressure was monitored

and regulated using two pressure regulators. A series of valves allowed the CO₂ to pass from the cylinder into the chamber and from the chamber into the limewater. A schematic diagram of the carbonation setup is shown in Figure 14.

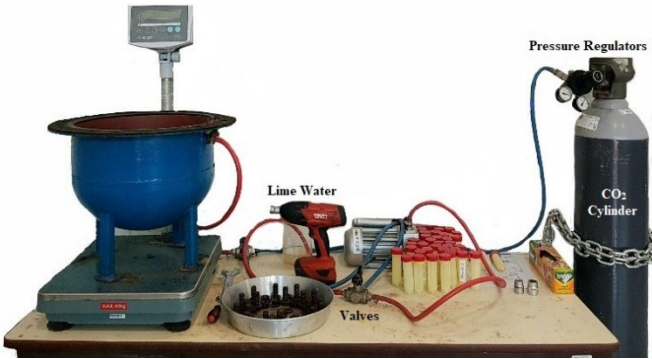


Figure 13: Carbonation setup

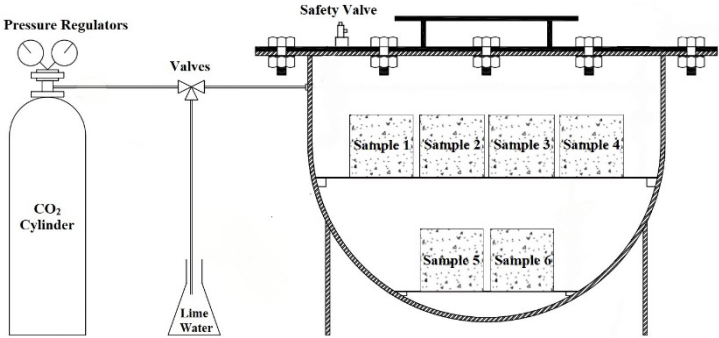


Figure 14: Schematic diagram of carbonation setup

2.4.4.3 Post-Carbonation Curing

After subjecting concrete samples to accelerated carbonation curing, they were cured following two post-carbonation curing techniques. The first method involved sealed subsequent hydration, where the cubes were kept in a sealed plastic bag till the testing age, as displayed in Figure 15a. Conversely, the second method entailed the compensation of the water lost during the initial curing and carbonation curing processes to study its impact on subsequent hydration until the age of 28 days as shown in Figure 15b. Water was

sprayed onto mix M4 (20a+4c-5P-6M) specimens until saturation every day for the first 7 days and every other day until 28 days. This mix was specifically selected for the post-carbonation curing as it had the highest CO₂ uptake within 24 hours timeframe and, therefore, had lost the most amount of water during the carbonation reaction. After each spraying step, the samples were placed in a sealed plastic bag. The process was repeated until testing age.



Figure 15: Post-carbonation curing techniques. (a) Sealed subsequent hydration and (b) water-sprayed hydration

2.4.5 Carbon Uptake

Two methods were used to quantify the CO₂ uptake of carbonated samples. The first method was mass gain. In this technique, the CO₂ uptake was estimated by comparing the mass of the specimens before and after carbonation. Three samples were used per mix to obtain an average CO₂ uptake. Since the carbonation process was a closed system, the water lost during the carbonation reaction was collected by absorbent paper and added to the final mass, as illustrated in Equation (1) [103].

$$\text{CO}_2 \text{ uptake (\%)} = \frac{\text{Final mass} + \text{Water mass} - \text{Initial mass}}{\text{Cement mass}} \times 100\% \tag{1}$$

The second method was the thermal decomposition analysis (TDA). A fractured sample was burnt per mix up to 550°C and 1000°C to quantitatively measure the bound water in hydration products and carbon dioxide in carbonates, respectively. The difference

in mass between 550°C and 1000°C represented the CO₂ uptake by carbonation, as clarified in Equation (2) [103].

$$\text{CO}_2 \text{ uptake (\%)} = \frac{\text{Mass at 550}^\circ\text{C} - \text{Mass at 1000}^\circ\text{C}}{\text{Cement mass}} \times 100\% \quad (2)$$

2.4.6 Phenolphthalein Carbonation Indicator

After the accelerated carbonation curing process, phenolphthalein solution was used to assess the average carbonation depth and identify the carbonated and uncarbonated regions of the carbonated and hydrated samples. It was sprayed on the freshly cut surfaces of the 28-day specimens of the mixes. The solution turned to violet/pink if the surface was uncarbonated, whereas it remained colorless when it was in contact with a carbonated surface.

2.4.7 Concrete Performance Evaluation

More than 120 samples were tested to evaluate and assess the different properties of the concrete mixes cast in this research. The experimental tests are described in the following sections.

2.4.7.1 Compressive Strength

The cube compressive strength of concrete was evaluated in accordance with BS EN-12390-3 at the age of 1, 7, and 28 days [104]. The test was conducted to assess the mechanical performance of the produced MOF-incorporating concrete. Three 50-mm cube samples were tested per mix to obtain an average compressive strength. An axial load was applied at a loading rate of 7 kN/s using an electro-hydraulic servo-controlled machine with a capacity of 2000 kN. The compressive strength was obtained using Equation (3). The test machine and tested cubes are shown in Figures 16 and 17, correspondingly.

$$\text{Compressive strength (MPa)} = \frac{\text{Maximum load applied}}{\text{Cross-sectional area}} \quad (3)$$



Figure 16: Compressive strength test machine



Figure 17: Tested cubes for compressive strength

2.4.7.2 Water Absorption and Permeable Pore Voids Volume

Water absorption and permeable pore voids volume of 1- and 28-day concrete samples were evaluated as per the procedure of ASTM C642 [105]. The tests were performed to examine the effect of incorporating MOF on the durability of concrete mix. The specimens were first oven-dried at a temperature of 105°C for 24 hours until a mass change of less than 0.5% was attained, as depicted in Figure 18. After cooling down to room temperature in a desiccator, the oven-dried mass (OD) was determined. The cubes were then immersed in water at approximately 21°C for 48 hours (Figure 19). To remove the surface moisture, the samples were surface-dried with a towel, and the saturated surface dry mass (SSD) was measured. The water absorption was then calculated using Equation (4).

$$\text{Water absorption (\%)} = \frac{\text{SSD} - \text{OD}}{\text{OD}} \times 100\% \quad (4)$$

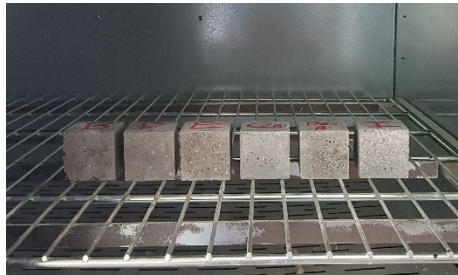


Figure 18: Oven-dried specimens for water absorption



Figure 19: Immersed cubes for water absorption

After oven-drying and attaining SSD state (i.e., following water absorption test), the samples were placed in a container, covered with tap water, and boiled for 5 hours, as displayed in Figure 20. After removing the samples and cooling them down to a temperature of 25°C, the surface moisture was removed with a towel, and the mass (BM) was measured. Finally, the cubes were suspended by a wire in water to determine the apparent mass (AM), as illustrated in Figure 21. The permeable pore voids volume was obtained using Equation (5).



Figure 20: Boiled samples for permeable voids pore volume



Figure 21: Suspended cubes for permeable voids pore volume

$$\text{Volume of permeable pore voids (\%)} = \frac{\text{BM} - \text{OD}}{\text{BM} - \text{AM}} \times 100\% \quad (5)$$

2.4.8 Microstructure Characterization

The microstructure of MOF-incorporating carbonated concrete was evaluated and compared to those of hydrated and carbonated counterparts without MOF. PXRD, SEM, and FTIR spectroscopy were performed to characterize the microstructure of 1- and 28-day samples of selected mixes. Mixes C0 (0a+0c-0P-0M), C1 (20a+4c-1P-0M), and M1-2 (20a+4c-1P-6M) were tested at 1 day to study the effect of carbonation and MOF incorporation on the microstructure of concrete. Meanwhile mixes C0 (0a+0c-0P-0M), M1-2 (20a+4c-1P-6M), M2 (4a+4c-1P-6M), M3 (20a+20c-1P-6M), C4 (20a+4c-5P-0M) and M4 (20a+4c-5P-6M) were evaluated at 28 days to evaluate the influence of different initial curing durations (M1-2 and M2), carbonation durations (M1-2 and M3), carbonation pressure (M1-2 and M4), sample age (M1-2 at 1 day and 28 days), and MOF content (C4 and M4).

2.4.8.1 Powder X-ray Diffraction Analysis (PXRD)

Powder XRD was conducted on powder samples that were obtained by crushing and grinding specimens tested for compressive strength. The patterns were obtained by means of a Philips PW1710 Powder Diffractometer (Cu, $K\alpha$ radiation, X'celerator proportional detector, scan interval 10–100°, 0.02°, and 0.5 s per step) to identify the phases of hydration and carbonation products in different concrete mixes.

2.4.8.2 Scanning Electron Microscope (SEM)

SEM was performed using a JEOL-JSM 6390A microscope, coupled with energy-dispersive X-ray (EDX) to observe and assess the effect of process parameters and MOF incorporation on the morphology and phases of different concrete mixes. Concrete chunks were extracted from the surface of the specimens after conducting the compressive strength test. The collected samples were polished and sputter-coated with a thin layer (2–5 nm) of 99.9% pure gold to ensure conductivity during the test without covering the surface morphology, as illustrated in Figure 22. The micrographs were used to identify the MOF, hydration products, and carbonation products in the concrete mixes.



Figure 22: Prepared samples for SEM

2.4.8.3 Fourier Transform Infrared (FTIR) Spectroscopy

FTIR was conducted using Nexus 470 FT-IR spectrometer at a resolution of 0.125 cm^{-1} from 400 to 4000 cm^{-1} (Figure 23). Powdered samples, similar to those used in the PXRD test, were interground with potassium bromide (KBr) at a powder sample-to-KBr ratio of 1:100, by mass, as shown in Figure 24.



Figure 23: FTIR spectrometer

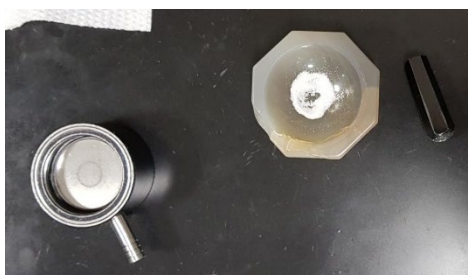


Figure 24: Interground sample with potassium bromide for FTIR

Chapter 3: Results and Discussions – Concrete Performance

3.1 Overview

This chapter highlights and discusses the main findings of this thesis. The mechanical properties and durability performance of the concrete mixes are assessed by means of the carbon uptake, phenolphthalein solution evaluation, compressive strength, water absorption, and permeable pore voids volume.

3.2 Carbon Uptake

The carbon uptake of concrete can be determined using numerous techniques, of which mass gain is the simplest [63-65]. To confirm its viability and accuracy in estimating the carbon uptake, it was compared to the thermal decomposition analysis (TDA). Table 6 shows the carbon uptake capacity determined by these two methods for selected mixes. For the mass gain, mixes C0, C2, and M1-2 had CO₂ uptakes of 0.00, 4.70, and 9.88%, respectively, by cement mass. Meanwhile, the TDA method entails two values, the CO₂ content and CO₂ uptake. The former considers all the carbonates in the sample, pre-existing and carbonation-induced. Therefore, the CO₂ uptake associated with carbonation curing was determined by subtracting the pre-existing carbonates from the CO₂ content. Comparing the results shows comparable CO₂ uptake capacities with respective TDA values of 0.00, 4.37, and 9.01%, by cement mass, for mixes C0, C2, and M1-2. This provides evidence of the ability to utilize mass gain as the sole technique for estimating the CO₂ uptake hereafter. Similar conclusions have been obtained in past work on the accelerated carbonation curing of concrete masonry units [63-65].

Table 6: Comparison of CO₂ uptake obtained from mass gain and TDA

Mix ID	Mix designation	Mass gain (%)	TDA, CO ₂ content (%)	TDA, CO ₂ uptake (%)
C0	0a+0c-0P-0M	0.00	2.71	0.00
C2	4a+4c-1P-0M	4.70	7.08	4.37
M1-2	20a+4c-1P-6M	9.88	11.72	9.01

Four different parameters critically affect the carbonation reaction and properties of concrete. These comprised initial air curing duration, accelerated carbonation curing duration, CO₂ pressure inside the chamber, and quantity of MOF. To evaluate the effect of each parameter, a total of 10 carbonated mixes and 1 hydrated control mix were examined. Figure 25 illustrates the CO₂ uptake, by cement mass, of the carbonated mixes.

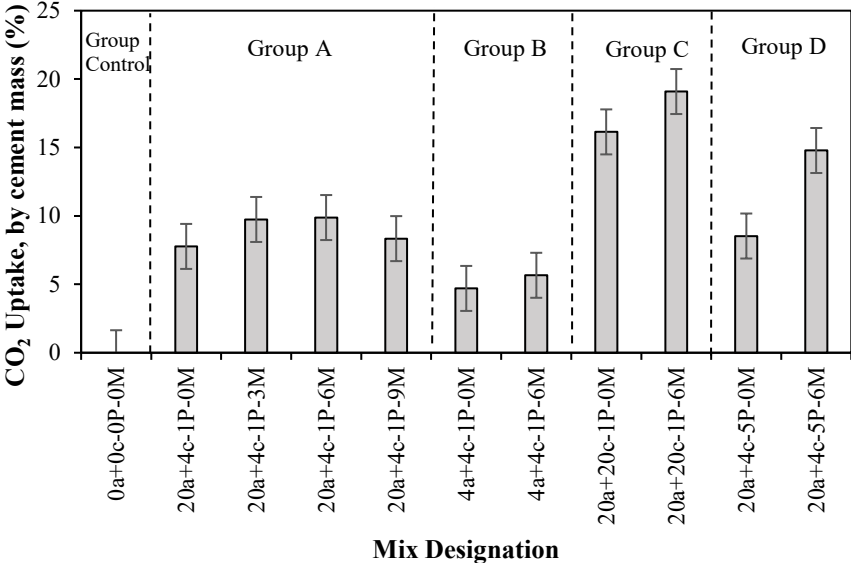


Figure 25: Carbon uptake percent by cement mass for concrete mixes

3.2.1 Effect of Quantity of MOF

Different percentages of MOF NH₂-MIL-125 (0, 3, 6, and 9%, by cement mass) were incorporated into the concrete to examine the effect of the quantity of MOF on the CO₂ uptake. For this study, mixes of Group A (i.e., 20a+4c-1P-0M, 20a+4c-1P-3M, 20a+4c-1P-6M, and 20a+4c-1P-9M) were compared, as shown in Figure 26. Increasing the MOF percentage from 0 to 3 and 6%, by cement mass, led to an increase in CO₂ uptake from 7.77 to 9.74 and 9.88%, respectively, representing respective 25 and 27% improvements in the carbonation efficiency. However, increasing the quantity of MOF to 9%, by cement mass, decreased the uptake to 8.34%. It is possible that increasing the MOF quantity beyond 6% may have caused agglomeration of the MOF particles inside the concrete, thus reducing the CO₂ adsorption sites and decreasing the uptake. Such agglomeration of NH₂-MIL-125 particles has been noticed when preparing a MOF

composite for photocatalysis [106]. Moreover, the effect of MOF inclusion on the CO₂ uptake of concrete can be evaluated by comparing the two mixes within each group. In fact, adding 6% MOF, by cement mass, to groups B, C, and D increased the CO₂ uptake by 20, 18, and 73%, respectively. These results provide evidence of the capability of MOFs to adsorb CO₂ gas and increase the CO₂ uptake of the concrete matrix.

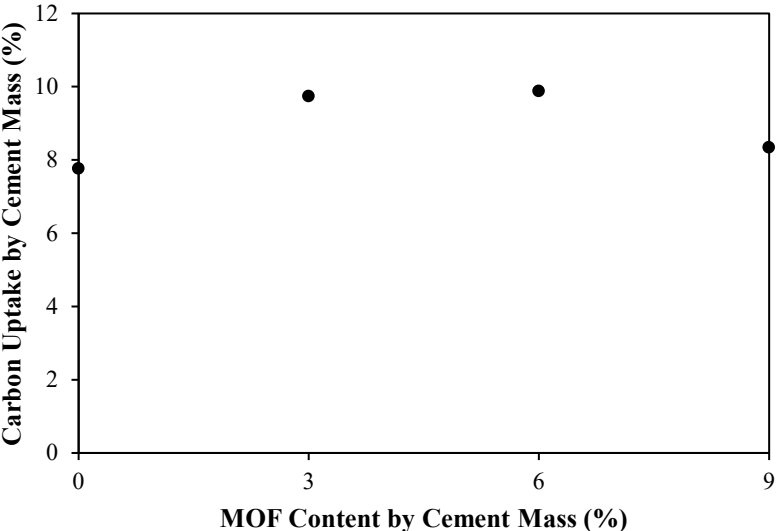


Figure 26: Carbon uptake by cement mass as a function of MOF content

The carbonation reaction efficiency of MOF is examined. Table 7 summarizes the results of carbonated concrete mixes. The total CO₂ uptake, by cement mass, are the same values as in Figure 25. For mixes without MOF, the total CO₂ uptake is attributed to the cement only and is, therefore, the same as the cement CO₂ uptake in these mixes. Meanwhile, for mixes with MOF, the cement CO₂ uptake is the same as those without MOF for each mix group. For instance, the cement CO₂ uptake of mix C1 (20a+4c-1P-0M) and M1-2 (20a+4c-1P-6M) is 7.77%. Yet, as noted earlier, the total CO₂ uptake of MOF-incorporating concrete was higher than that of mixes without MOF. As such, the remaining uptake was associated with the MOF, designed by MOF CO₂ uptake (column 5 in Table 7). This value was converted into carbonation reaction efficiency in a two-step process. First, the CO₂ mass (kg/m³) was calculated by multiplying the MOF CO₂ uptake (%) by the mass of cement (kg/m³). Then, the carbonation reaction (mg/g) efficiency is

determined by dividing the CO₂ mass (kg/m³) by the mass of the MOF (kg/m³). The highest MOF reaction efficiency was that of mix M4 (20a+4c-5P-6M) with a value of 1041.67 mg/g, followed by mixes M1-1 (20a+4c-1P-3M) and M3 (20a+20c-1P-6M) with respective efficiencies of 655.88 and 491.67 mg/g. Furthermore, a comparison between mixes M1-1 (20a+4c-1P-3M) and M1-2 (20a+4c-1P-6M) showed that the former had a lower uptake but higher reaction efficiency than the latter. Apparently, adding two times more MOF in the latter (M1-2) reduced the reaction efficiency, owing to possible agglomeration of the MOF particles. In fact, if the efficiency was unaffected by the total mass of MOF added to the mix, the total CO₂ uptake would have reached 11.71%.

Table 7: Carbonation reaction measurements of concrete mixes

Mix ID	Mix designation	Total CO ₂ uptake (%)	Cement CO ₂ uptake (%)	MOF			Corrected cement CO ₂ uptake (%)
				CO ₂ uptake (%)	CO ₂ mass (kg/m ³)	Reaction efficiency (mg/g)	
C1	20a+4c-1P-0M	7.77 ± 0.3	7.77	-	-	-	-
M1-1	20a+4c-1P-3M	9.74 ± 0.1	7.77	1.97	6.69	655.88	9.33
M1-2	20a+4c-1P-6M	9.88 ± 0.2	7.77	2.11	7.17	351.47	9.06
M1-3	20a+4c-1P-9M	8.34 ± 0.3	7.77	0.57	1.94	63.40	-
C2	4a+4c-1P-0M	4.70 ± 0.1	4.70	-	-	-	-
M2	4a+4c-1P-6M	5.66 ± 0.1	4.70	0.96	3.26	159.80	4.84
C3	20a+20c-1P-0M	16.14 ± 0.6	16.14	-	-	-	-
M3	20a+20c-1P-6M	19.09 ± 0.7	16.14	2.95	10.03	491.67	18.27
C4	20a+4c-5P-0M	8.53 ± 0.3	8.53	-	-	-	-
M4	20a+4c-5P-6M	14.78 ± 0.7	8.53	6.25	21.25	1041.67	13.96

Based on past literature, the CO₂ adsorption capacity of NH₂-MIL-125 was up to 136 mg/g [99]. In this work, the MOF was placed in the CO₂ chamber at a temperature of 25°C and RH of 50% for up to 4 days. The CO₂ uptake did not exceed 12.5%, by MOF mass, or a reaction efficiency of 125 mg/g. Whether the value from past literature or this work is considered, the obtained carbonation reaction efficiency for mixes M1-1 (20a+4c-1P-3M), M1-2 (20a+4c-1P-6M), M2 (4a+4c-1P-6M), M3 (20a+20c-1P-6M), and M4 (20a+4c-5P-6M) was significantly higher. Since the MOF has a specific adsorption capacity based on its chemical and physical properties, the excess CO₂ was, in fact, captured by the cement. For this reason, a corrected cement CO₂ uptake is calculated (column 8 in Table 7). Using the actual reaction efficiency of the NH₂-MIL-125 MOF

(136 mg/g), the actual mass of CO₂ attributed to the MOF was calculated. The MOF CO₂ uptake was then calculated as a function of the mass of cement and subtracted from the total CO₂ uptake to calculate the corrected cement CO₂ uptake. The corrected cement CO₂ uptake was higher than the originally considered cement CO₂ uptake, assumed to be equal to that of mixes without MOF from the same group, by up to 64%. This shows that not only does the addition of MOF to the concrete increase the CO₂ uptake through adsorption to the MOF, but it also promotes a higher degree of carbonation of the cement, evidenced by the higher cement CO₂ uptake than that in mixes without MOF.

3.2.2 Effect of Initial Curing Duration

Four concrete mixes were considered in the evaluation of the effect of initial curing on the degree of carbonation reaction, namely C2 (4a+4c-1P-0M), C1 (20a+4c-1P-0M), M2 (4a+4c-1P-6M), and M1-2 (20a+4c-1P-6M), as shown in Figure 27. These mixes were carbonated under a constant pressure of 1 bar and for a duration of 4 hours. For the first two mixes without the MOF (i.e., 4a+4c-1P-0M and 20a+4c-1P-0M), extending the initial curing duration from 4 to 20 hours increased the CO₂ uptake from 4.70 to 7.77%, representing an increase of 65%. Meanwhile, for mixes incorporating MOF (i.e., 4a+4c-1P-6M and 20a+4c-1P-6M), the CO₂ uptake increased by 75%, from 5.66 to 9.88%. Apparently, prolonging initial curing had a more prominent impact on the degree of carbonation reaction for mixes incorporating MOF.

The enhancement in the degree of carbon reaction due to initial curing was interpreted. After 4 hours of initial curing, the concrete surface was still saturated as a result of the excess free water in the mix. It is also possible that the MOF had adsorbed water, as earlier research had confirmed the water adsorption potential of NH₂-MIL-125 [107]. These two phenomena hindered the respective carbonation reaction with cement and adsorption of CO₂ by the MOF. Increasing the initial curing duration to 20 hours drove out part of the excess free water from the concrete and MOF, thus creating voids that facilitated the diffusion of the CO₂ gas into the specimen. Consequently, the diffused CO₂ reacted with the cement and was adsorbed by the MOF, achieving a higher carbonation degree. A similar effect of initial curing on the degree of carbonation was noted in a previous study on the carbonation of conventional concrete incorporating limestone powder [108].

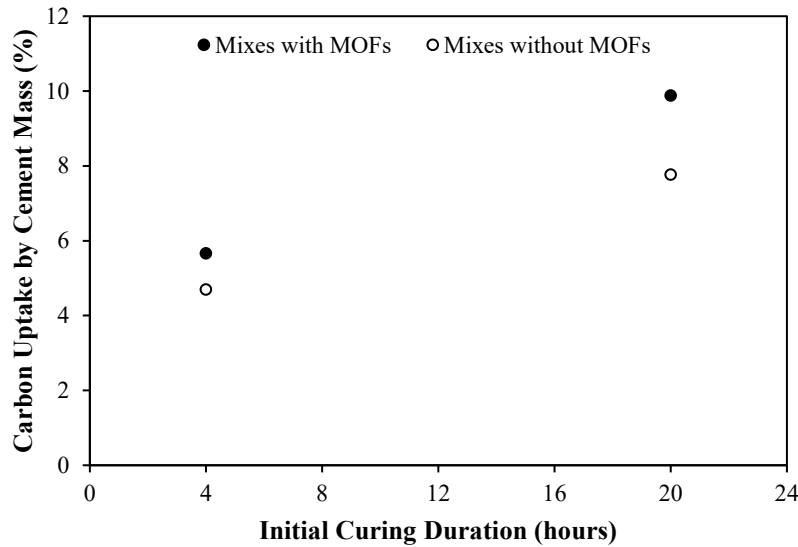


Figure 27: Carbon uptake by cement mass as a function of initial curing duration

Furthermore, in section 3.2.1, it was found that the addition of the MOF promoted the carbonation of cement and increased its affiliated CO₂ uptake. In fact, as shown in Table 7, after correction, the cement CO₂ uptake increased from 4.70 to 4.84% (corrected) and 7.77 to 9.06% (corrected) for mixes C1 (4a+4c-1P-6M) and M1-2 (20a+4c-1P-6M), representing increases of 3 and 17%, respectively. This signifies that the extent of improvement in the carbonation of cement (i.e., cement CO₂ uptake) due to the addition of MOF is more pronounced with longer initial curing durations.

3.2.3 Effect of Accelerated Carbonation Duration

The effect of accelerated carbonation duration on the CO₂ sequestration capacity is demonstrated in Figure 28 by comparing mixes C1 (20a+4c-1P-0M), C3 (20a+20c-1P-0M), M1-2 (20a+4c-1P-6M), and M3 (20a+20c-1P-6M). The curing regime for these mixes entailed 20 hours of air curing followed by carbonation at a pressure of 1 bar. For mixes without MOF, increasing the carbonation duration from 4 to 20 hours increased the CO₂ uptake from 7.77 to 16.14%, signifying an increase of 108%. Comparably, a longer carbonation period of mixes incorporating 6% of the MOF enhanced the CO₂ uptake by 93%, from 9.88 to 19.09%. Apparently, extending the carbonation duration prolonged cement exposure to CO₂ gas and consequently promoted higher carbon uptake. Past work reported similar findings, where the carbonation of lightweight expanded slag concrete for

4 and 18 hours resulted in CO₂ uptakes of 13 and 20%, respectively [66]. Furthermore, the inclusion of MOF in carbonation-cured concrete improved the carbonation reactivity of cement by up to 17%. Yet, it seems that the extent of this improvement was not significantly impacted by the extension of the carbonation duration from 4 to 20 hours.

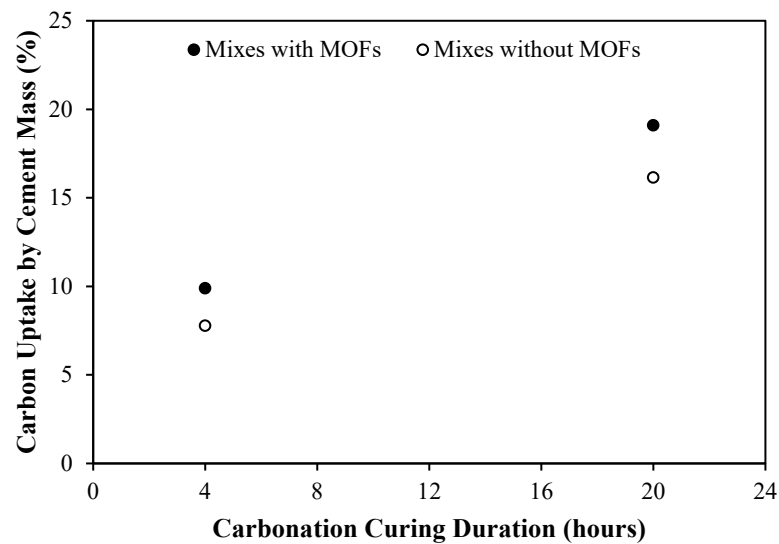


Figure 28: Carbon uptake by cement mass as a function of carbonation curing duration

3.2.4 Effect of CO₂ Pressure

The relationship between the pressure during carbonation and CO₂ uptake is demonstrated by comparing mixes C1 (20a+4c-1P-0M), C4 (20a+4c-5P-0M), M1-2 (20a+4c-1P-6M), and M4 (20a+4c-5P-6M), as shown in Figure 29. Mixes made without MOF and carbonated at pressures of 1 and 5 bars had carbon uptakes of 7.77 and 8.53%, respectively. Indeed, such an increase in pressure led to a 10% increase in uptake. Meanwhile, increasing the pressure while carbonating MOF-incorporating mixes led to respective carbon uptakes of 9.88% and 14.78%, representing an increase of 50%. Clearly, higher pressure promoted a higher degree of carbonation, as it allowed for deeper penetration and diffusion of CO₂ into the concrete and MOF. Yet, the level of increase in CO₂ uptake due to elevated pressure was higher in mixes incorporating MOF. Moreover, the cement CO₂ uptake increased by 17 and 64% when MOF-incorporating mixes were carbonated at pressures of 1 and 5 bars, respectively. This shows that the improvement in

the carbonation reactivity of cement due to the addition of MOF was more pronounced at higher pressures.

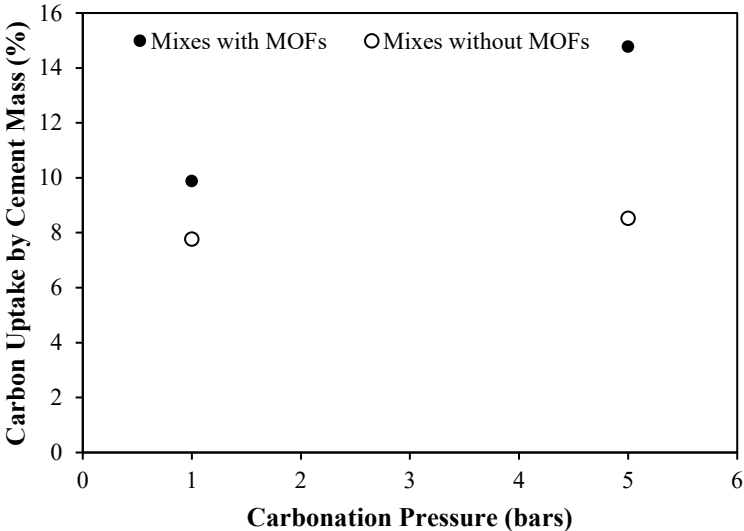


Figure 29: Carbon uptake by cement mass as a function of carbonation pressure

3.3 Phenolphthalein Solution Evaluation

Figure 30 shows the carbonated and uncarbonated regions of the concrete mixes. The average carbonation depth was assessed by spraying the freshly cut concrete surface with the phenolphthalein solution. The less basic regions, with a pH lesser than 9, remained colorless to a bright pink color, signifying the progress of the carbonation reaction. Meanwhile, the more basic regions, with a pH of more than 9, turned into a pink or magenta color. Table 8 illustrates the average carbonation depths of the concrete mixes.

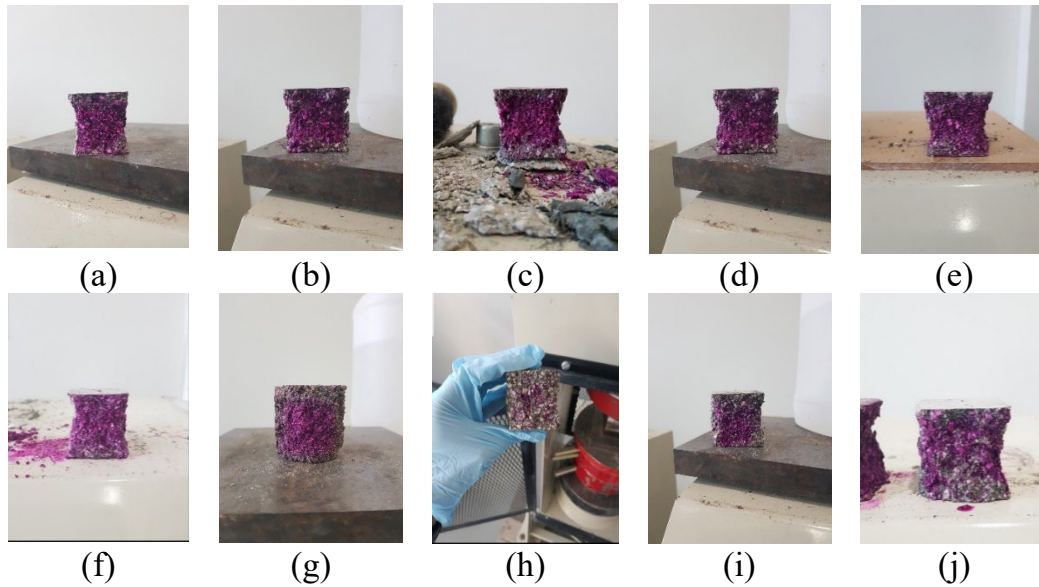


Figure 30: Images of samples sprayed with phenolphthalein indicator solution. (a) C1, (b) M1-1, (c) M1-2, (d) M1-3, (e) C2, (f) M2, (g) C3, (h) M3, (i) C4, (j) M4

Incorporating MOF in concrete mixes increased the average carbonation depth. This is well-aligned with the increases in CO₂ uptake. Adding MOF by 3, 6, and 9%, by cement mass, in group A led to increases in the depth of 35, 39, and 8%, respectively. Meanwhile, the inclusion of 6% MOF, by cement mass, in groups B, C, and D resulted in a 7, 18, and 58% increase in the depth of carbonation, correspondingly.

The effect of initial curing on the average carbonation depth was examined by comparing mixes 4a+4c-1P-0M, 20a+4c-1P-0M, 4a+4c-1P-6M, and 20a+4c-1P-6M. The mixes made without MOF experienced an increase of 14% in carbonation depth, from 4.3 to 4.9 mm, upon extending the initial curing duration to 20 hours. This finding is associated with a 65% increase in CO₂ uptake. Conversely, for mixes incorporating MOF (i.e., 4a+4c-1P-6M and 20a+4c-1P-6M), the respective increase in depth reached 48%, as shown in Figure 30, corresponding to a 75% increase in CO₂ uptake. Clearly, initial curing was more impactful on the carbonation efficiency of mixes made with MOF.

Table 8: Average carbonation depths of concrete mixes at 28 days

Mix ID	Mix designation	Total CO ₂ uptake (%)	Average carbonation depth (mm)
C1	20a+4c-1P-0M	7.77 ± 0.3	4.9 ± 0.2
M1-1	20a+4c-1P-3M	9.74 ± 0.1	6.6 ± 1.1
M1-2	20a+4c-1P-6M	9.88 ± 0.2	6.8 ± 1.0
M1-3	20a+4c-1P-9M	8.34 ± 0.3	5.3 ± 0.8
C2	4a+4c-1P-0M	4.70 ± 0.1	4.3 ± 0.7
M2	4a+4c-1P-6M	5.66 ± 0.1	4.6 ± 0.8
C3	20a+20c-1P-0M	16.14 ± 0.6	9.8 ± 1.2
M3	20a+20c-1P-6M	19.09 ± 0.7	11.6 ± 1.3
C4	20a+4c-5P-0M	8.53 ± 0.3	5.9 ± 1.0
M4	20a+4c-5P-6M	14.78 ± 0.7	9.3 ± 1.2

Moreover, extending the carbonation curing duration from 4 to 20 hours for mixes without MOF (20a+4c-1P-0M and 20a+20c-1P-0M) increased the carbonation depth from 4.9 to 9.8 mm (100% increase), which is associated with a 108% increase in CO₂ uptake. Meanwhile, adding MOF to the concrete, as illustrated in Table 8, led to an increase of 71% in carbonation depth, from 6.8 to 11.6 mm, with an increase of 93% in uptake. This shows that prolonged carbonation curing is slightly more effective in mixes without MOF.

Furthermore, using a higher pressure for accelerated carbonation curing also had an impact on the average carbonation depth. For mixes made without MOF, the depth reached 5.9 mm, with respective increases in carbonation depth and CO₂ uptake of 20 and 10%. However, increasing the pressure to 5 bars in mix M4 (20a+4c-5P-6M) caused corresponding carbonation depth and CO₂ uptake increases of 37 and 50%. It is apparent that increasing the carbonation pressure had a significant impact on the degree of reaction in MOF-incorporating concrete mixes.

3.4 Compressive Strength

Figure 31 depicts the 1-, 7- and 28-day compressive strength of concrete mixes. Generally, the compressive strength of most concrete mixes without MOF improved upon accelerated carbonation curing in comparison with that of the hydrated control mix C0. Indeed, the largest improvements were recorded at the age of 1 day, reaching up to 30%. As carbonation is accelerated hydration, it converts calcium silicates in the unhydrated cement into calcium silicate hydrate and calcium carbonate [64-66]. The formation of these carbonation products led to a reduction in the porosity by filling the pores in the

cement matrix, thus enhancing the compressive strength [108-110]. Meanwhile, their 7- and 28-day compressive strengths were up to 16 and 17% higher than the hydrated control mix C0. On the other hand, concrete mixes incorporating MOF had varying 1-day strengths ranging between 46% lower to 16% higher than that of the hydrated control mix. Yet, this variation reduced with age, with 7- and 28-day strengths being 5% less to 30% more than those of mix C0. It seems that the addition of MOF may have affected the early-age compressive strength, especially for mixes that had a short initial curing duration of 4 hours and high MOF content of 9%. Nevertheless, this negative impact was reduced with subsequent hydration.

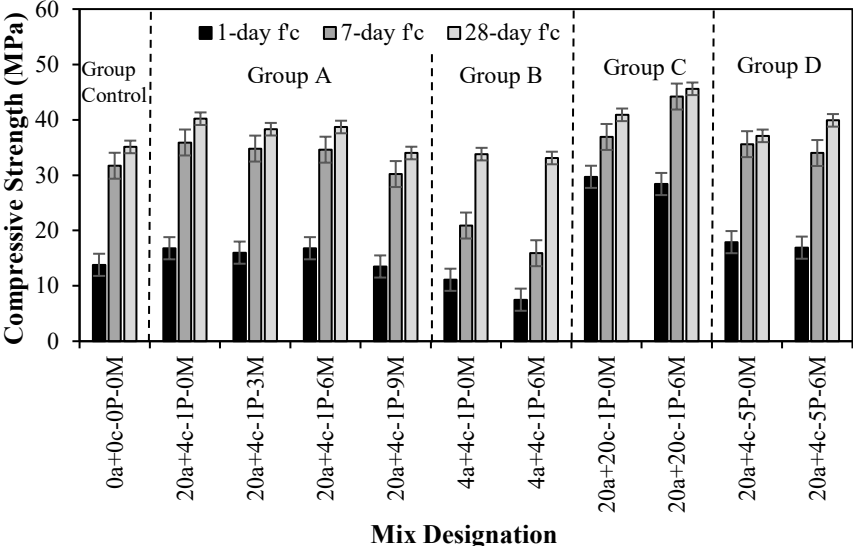


Figure 31: Compressive strength of concrete mixes

Table 9: Strength gain of concrete over time

Mix ID	Mix designation	Compressive strength (MPa)			Strength gain (%)	
		1-day	7-day	28-day	1 to 7	7 to 28
C0	0a+0c-0P-0M	13.8	31.7	35.1	130.1	10.7
C1	20a+4c-1P-0M	16.8	35.9	40.2	113.8	12.0
M1-1	20a+4c-1P-3M	16.0	34.8	38.3	118.0	10.1
M1-2	20a+4c-1P-6M	16.8	34.6	38.7	106.0	11.8
M1-3	20a+4c-1P-9M	13.5	30.2	34.0	123.6	12.5
C2	4a+4c-1P-0M	11.1	20.9	33.8	88.0	61.7
M2	4a+4c-1P-6M	7.5	15.9	33.1	112.3	108.6
C3	20a+20c-1P-0M	29.7*	36.9	40.9	24.2	11.0
M3	20a+20c-1P-6M	28.4*	44.2	45.6	55.9	3.1
C4	20a+4c-5P-0M	17.9	35.6	37.1	99.6	4.0
M4	20a+4c-5P-6M	16.9	34.0	39.9	101.2	17.2

*2-day compressive strength.

The strength gain profile of concrete mixes is shown in Table 9. Of the mixes made without MOF, the hydrated control C0 had the highest strength gain up to 7 days, while the lowest was for mix 20a+20c-1P-0M. Apparently, the strength development associated with the hydration reaction in C0 progressed rapidly within the first 7 days, after which it decelerated until 28 days. As for mix 20a+20c-1P-0M, it should be noted that the sample was tested at the age of 2 days, as 20-hour initial curing was succeeded by another 20 hours of carbonation curing. In this mix, nearly 73% of the 28-day strength was attained at the age of 2 days, owing to the accelerated hydration reaction induced by prolonged 20-hour carbonation curing. This resulted in the lowest strength gain up to 7 days. Conversely, MOF-incorporating mixes had superior strength gain from 1 to 7 days compared to counterparts mixes without MOF, except for mix M1-2. Yet, among such mixes, those with the lowest 1-day strength had the highest gain over the first 7 days. These results indicate that the inclusion of MOF in concrete does not hinder the hydration reaction. However, the process parameters and inclusion of MOF in the concrete have impacted the compressive strength. The following sections discuss the effect of each process parameter and quantity of MOF on the concrete compressive strength.

3.4.1 Effect of MOF Quantity

The effect of MOF quantity on the compressive strength was primarily investigated through the Group A mixes (20a+4c-1P-0M, 20a+4c-1P-3M, 20a+4c-1P-6M, and 20a+4c-

1P-9M). The mixes incorporating MOF had respective 1-day strength values of 16.0, 16.8, and 13.5 MPa. The impact of incorporating MOF was only apparent with 9% MOF content, by cement mass. It seems that the agglomeration of MOF in the concrete may have not only affected the carbonation reaction efficiency, i.e., carbon uptake capacity, but also the early-age compressive strength.

Nevertheless, the negative impact of MOF addition on compressive strength was diminished over time, with 5, 3, and 15% losses in 28-day strengths for mixes made with 3, 6, and 9% MOFs. As such, the optimum quantity of MOF, from an uptake and strength point of view, was 6%, by cement mass, and thus was employed in further analysis. Yet, a MOF content of 3% could also be used in future work, owing to its superior uptake capacity and comparable strength results to those of the carbonated mix without MOF (20a+4c-1P-0M). Moreover, it is worth noting that the 28-day strengths of MOF-incorporating concrete mixes were comparable or superior to those of the hydrated control mix C0.

The effect of MOF inclusion on the 28-day compressive strength of concrete can also be evaluated by comparing the two mixes within groups B, C, and D. The addition of 6% MOF, by cement mass, in group B mixes (4a+4c-1P-0M and 4a+4c-1P-6M) resulted in an insignificant decrease in strength (2%), while in groups C and D, the strength increased by 11 and 8%, respectively. These results highlight the feasibility of adding MOFs to enhance the carbon uptake capacity of concrete while either improving or not significantly affecting concrete mechanical performance.

3.4.2 Effect of Initial Curing Duration

The effect of the initial curing duration on the compressive strength of concrete made with and without MOF was assessed using four concrete mixes, namely C2 (4a+4c-1P-0M), C1 (20a+4c-1P-0M), M2 (4a+4c-1P-6M), and M1-2 (20a+4c-1P-6M). These mixes were carbonated under a constant pressure of 1 bar and for a duration of 4 hours. Mixes without MOF (i.e., 4a+4c-1P-0M and 20a+4c-1P-0M) experienced increases of 51, 72, and 19% in 1-, 7-, and 28-day compressive strength upon extending the initial curing duration from 4 to 20 hours. This is associated with a 65% increase in CO₂ uptake. Past work highlighted that higher CO₂ uptake resulted in the formation of more carbonation products, densification of the matrix, and higher compressive strength [111, 112].

For mixes incorporating MOF (i.e., 4a+4c-1P-6M and 20a+4c-1P-6M), the respective compressive strength at 1, 7, and 28 days increased by 125, 118, and 17% when initial curing increased from 4 to 20 hours. Under the same conditions, the CO₂ uptake increased by 75%. Clearly, the extension of initial curing was more impactful on the performance of concrete mixes made with MOF. Nevertheless, noteworthy is that the strength increased by the least percentage (17%) at the age of 28 days, owing to the water loss during the initial curing and carbonation phases. As this water was not compensated for in sealed air curing, the subsequent hydration reaction was hindered, thus reducing the degree of hydration and compressive strength. However, this strength could be improved by subsequent spraying, as noted in earlier work [64]. A similar attempt was made in this work, whereby mix M4 (20a+4c-5P-6M) was sprayed, as per the procedure of section 2.4.4.3. As a result, the 28-day compressive strength increased from 39.9 to 43.1 MPa, representing an increase of 8%. Water spraying after carbonation facilitated the formation of hydration products, thus improving the compressive strength.

3.4.3 Effect of Accelerated Carbonation Curing Duration

The effect of accelerated carbonation duration on the compressive strength of concrete was assessed using mixes C1 (20a+4c-1P-0M), C3 (20a+20c-1P-0M), M1-2 (20a+4c-1P-6M), and M3 (20a+20c-1P-6M). Their curing scheme entailed 20 hours of initial curing followed by carbonation at a pressure of 1 bar. Since the second and fourth mixes could not be tested at the age of 1 day, the comparison was made for 7 and 28 days only. Mixes made without MOF exhibited insignificant increases (<3%) in 7- and 28-day strengths upon extending carbonation curing from 4 to 20 hours. Despite an increase of 108% in the uptake, the strength was not improved. It seems that uncarbonated cement in mix C1 (20a+4c-1P-0M) may have hydrated during the subsequent hydration phase, creating more hydration products.

For the mixes incorporating MOF (20a+4c-1P-6M and 20a+20c-1P-6M), it was observed that the 7- and 28-day compressive strengths were enhanced by 28% and 18%, respectively. Prolonging carbonation curing led to higher CO₂ uptake, forming more carbonation products that occupy the microstructure, decrease the porosity, and enhance the compressive strength. As a result, the highest compressive strength was that of mix

M3 (20a+20c-1P-6M) with a value of 45.6 MPa. However, considering a 24-hour industrial time frame, the highest strength was that of mix M4 (20a+4c-5P-6M).

3.4.4 Effect of CO₂ Pressure

The effect of carbonation pressure on the compressive strength of concrete made with and without MOF is demonstrated by comparing mixes C1 (20a+4c-1P-0M), C4 (20a+4c-5P-0M), M1-2 (20a+4c-1P-6M), and M4 (20a+4c-5P-6M). Increasing the carbonation pressure from 1 to 5 bars led to a limited change in the compressive strengths of mixes made without MOF, which aligns with the limited increase in the carbon uptake. Indeed, the 1-day strength increased by 6%, while the 7- and 28-day strengths decreased by 1 and 7%. The carbonation regime led to accelerated hydration and the formation of carbonation and hydration products, which led to improved strength at an early age. However, the carbonation-induced water loss hindered the subsequent hydration reaction, resulting in lower 28-day strength.

Meanwhile, increasing the pressure during carbonation of MOF-incorporating mixes led to an insignificant change in the compressive strengths at 1 and 7 days and up to 3% at 28 days. Despite the higher carbon uptake at 5 bars, this was not reflected as an improvement in the compressive strength. More carbon uptake may have produced more carbonation products but may not have improved the cement-aggregate interfacial transition zone (ITZ), which predominantly controls the compressive strength of concrete [113, 114].

3.5 Water Absorption and Permeable Pore Voids Volume

The water absorption and permeable pore voids volume of 28-day concrete mixes are presented in Table 10. Increasing the quantity of MOF in the concrete mix generally increased these two properties. Indeed, the water absorption of mixes made with 0, 3, 6, and 9% MOF were 4.92, 5.22, 5.15, and 5.28%, respectively, while the corresponding permeable voids were 14.37, 14.97, 14.88, and 15.00%. These results are well-aligned with the compressive strength, whereby the addition of MOF caused a decrease in strength, with 6% MOF being superior to 3 and 9%. Apparently, adding MOF to concrete may create more voids, resulting in higher water absorption and lower compressive strength, as shown in Figure 32. However, these voids may have facilitated the diffusion of CO₂

into the MOF-incorporating concrete and promoted higher CO₂ uptake by the cement (Figure 33).

The effect of initial curing duration on these two characteristics was also examined. Extending initial curing from 4 to 20 hours for mixes without MOF reduced the water absorption and voids by 14 and 12%, respectively. Conversely, mixes with MOF experienced respective decreases of 9 and 5%. These results provide evidence of the densification of the concrete structure due to carbonation curing, thereby explaining the increase in 28-day compressive strength.

Moreover, extending the carbonation curing period from 4 to 20 hours led to a reduction in the water absorption and permeable pore voids volume. In fact, respective properties decreased by 8 and 17% for mixes without MOF and 17 and 23% for counterparts made with MOF, indicating that the extent of improvement in the resistance to water absorption due to prolonged carbonation is greater upon the addition of MOF. Ultimately, mixes carbonated for longer durations and inclusive of MOF were characterized by higher carbonation degree, lower water absorption, denser matrix, and higher compressive strength, as illustrated in Figures 32 and 33.

Table 10: Water absorption and permeable pore voids volume at 28 days

Mix ID	Mix designation	Water absorption (%)	Permeable pore voids volume (%)
C0	0a+0c-0P-0M	5.27 ± 0.42	13.89 ± 1.23
C1	20a+4c-1P-0M	4.92 ± 0.41	14.37 ± 1.11
M1-1	20a+4c-1P-3M	5.22 ± 0.39	14.97 ± 1.41
M1-2	20a+4c-1P-6M	5.15 ± 0.35	14.88 ± 1.38
M1-3	20a+4c-1P-9M	5.28 ± 0.42	15.00 ± 1.39
C2	4a+4c-1P-0M	5.75 ± 0.41	16.39 ± 1.41
M2	4a+4c-1P-6M	5.67 ± 0.55	15.69 ± 1.40
C3	20a+20c-1P-0M	4.55 ± 0.40	11.99 ± 0.98
M3	20a+20c-1P-6M	4.28 ± 0.41	11.46 ± 0.85
C4	20a+4c-5P-0M	4.86 ± 0.41	14.69 ± 1.10
M4	20a+4c-5P-6M	4.71 ± 0.50	12.43 ± 1.05

Furthermore, using a higher pressure for the accelerated carbonation curing regime had a limited impact on the water absorption and permeable voids, as was the case with compressive strength, decreased the absorption and voids percentages for mix C4 and M4. Meanwhile, adding MOF to the concrete along with higher pressure carbonation curing caused a reduction in the water absorption and voids volume by 9 and 17%, respectively, attributed to a higher degree of carbonation. This produced concrete with slightly higher 28-day compressive strength.

Moreover, spraying the concrete after carbonation reduced the water absorption and permeable voids by up to 2% and increased the strength by nearly 8%. This slight improvement in mechanical and physical properties is owed to the formation of more hydration products. Similar findings were obtained in past research on carbonated concrete made with Portland limestone cement [64].

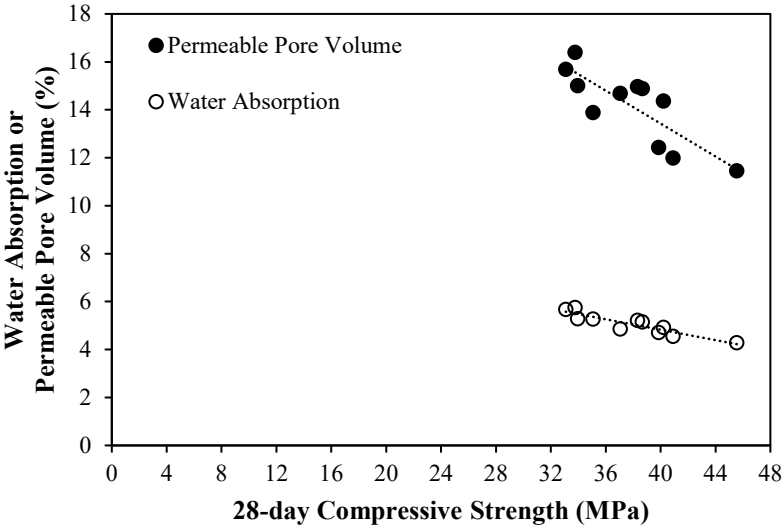


Figure 32: Correlation between 28-day compressive strength and each of water absorption and permeable pore volume

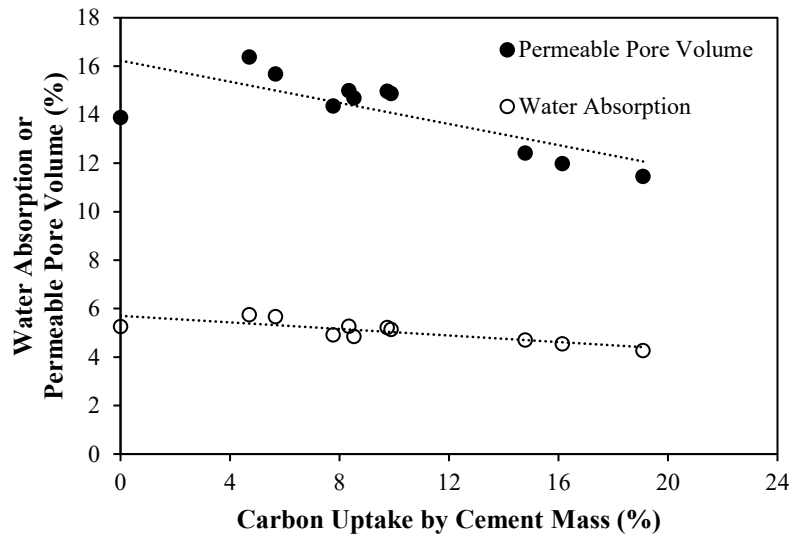


Figure 33: Correlation between carbon uptake by cement mass and each of water absorption and permeable pore volume

Chapter 4: Results and Discussion – Microstructural Characterization

4.1 Overview

This chapter displays and discusses the microstructure and morphological findings of the carbonated MOF-incorporating concrete mixes under different conditions in comparison to a hydrated reference mix. The microstructure tests were conducted in a way to assess the effects of concrete age, MOF quantity, initial curing duration, carbonation duration, carbonation pressure, and post-carbonation spraying on the phase composition, morphology, and microstructure of concrete. Mixes C0, C1, and M1-2 were tested at 1 day, whereas C0, M2, M1-2, M3, C4, and M4 were examined at 28 days.

4.2 Experimental Results

4.2.1 Powder X-ray Diffraction (PXRD) Analysis

To characterize the phase composition of the hydrated and carbonated concretes, the PXRD patterns were acquired at 1 and 28 days, as demonstrated in Figures 34 and 35, respectively. The diffraction peaks have been identified by the software and cross-checked against several previous works of literature [64, 65, 115, 116]. In the 1-day hydrated control mix, C0 (0a+0c-0P-0M), C₃S, C₂S, C-S-H, and ettringite peaks were observed. Similar phases have been reported in other work [116]. Conversely, the carbonated mix without MOF, C1 (20a+4c-1P-0M), showed newly-formed calcite peaks and a more intense C-S-H peak compared to the hydrated control. This highlights that carbonation is indeed an accelerated hydration reaction and provides evidence of the higher 1-day compressive strength, as presented in Table 9. For carbonated concrete mix made with MOF, M1-2 (20a+4c-1P-6M), the calcite and C-S-H peaks were significantly higher than those of counterpart mix without MOF. This is well-aligned with the increases in CO₂ uptake and compressive strengths due to MOF incorporation reported in sections 3.2 and 3.4. Also, the peaks of calcium silicates (C₃S and C₂S) have reduced or disappeared, indicating their partially or complete consumption during accelerated carbonation curing. Noteworthy is the presence of ettringite in all 1-day mixes. Apparently, its formation was independent of the curing regime and the presence of MOF. In addition, the calcium hydroxide (CH) peaks were absent in all mixes, owing to the possible formation of poorly

crystalline CH, as noted in other work on the effect of temperature and water-solid ratio on the growth of CH [117].

Furthermore, in the 28-day samples (Figure 35), the CH peak at $18^\circ 2\theta$ was distinctive in the hydrated reference mix C0. Apparently, CH formed during the 27-day subsequent hydration of cement. Yet, this peak was also noted for mix M2 (4a+4c-1P-6M), having the lowest carbonation degree. It seems that uncarbonated cement particles may have hydrated over time to form CH. Also, among all carbonated mixes, M2 had the lowest calcite and C-S-H peaks, providing evidence of its inferior CO₂ uptake (5.66%) and 28-day compressive strength (33.8 MPa).

To evaluate the impact of initial curing duration on the phase composition, mixes M2 (4a+4c-1P-6M) and M1-2 (20a+4c-1P-6M) were compared. It can be observed that the intensity of the calcite peak at $29.4^\circ 2\theta$ was higher in the latter mix, signifying a higher uptake with longer initial curing. This was consistent with the carbon uptake observations. Moreover, extending the carbonation duration to 20 hours in mix M3 (20a+20c-1P-6M) led to higher calcite and C-S-H peaks, which correlates to its high CO₂ uptake and 28-day compressive strength. Meanwhile, increasing the pressure to 5 bars in mix M4 (20a+4c-5P-6M) led to slightly higher calcite peaks compared to the counterpart carbonated at 1 bar but reported the formation of aragonite. A previous study concerning the reaction between hydrated Portland cement and supercritical CO₂ showed that higher carbonation pressure led to an increase in the amount of aragonite [118]. Yet, aragonite was not clearly observed in mix C4 (20a+4c-5P-0M), which may be due to its conversion to the more stable calcium carbonate polymorph, calcite. Past work on the carbonation of cement-based masonry blocks reported a similar transformation of aragonite into calcite [65]. As such, the presence of MOF in the concrete mix may have contributed to maintaining the aragonite in its typical form.

1: Calcite - CaCO_3 2: Tricalcium Silicate - C_3S 3: Dicalcium Silicate - C_2S
4: Calcium Silicate Hydrate - C-S-H E: Ettringite - $\text{Ca}_6\text{Al}_2(\text{SO}_4)_3(\text{OH})_{12}\cdot 26\text{H}_2\text{O}$

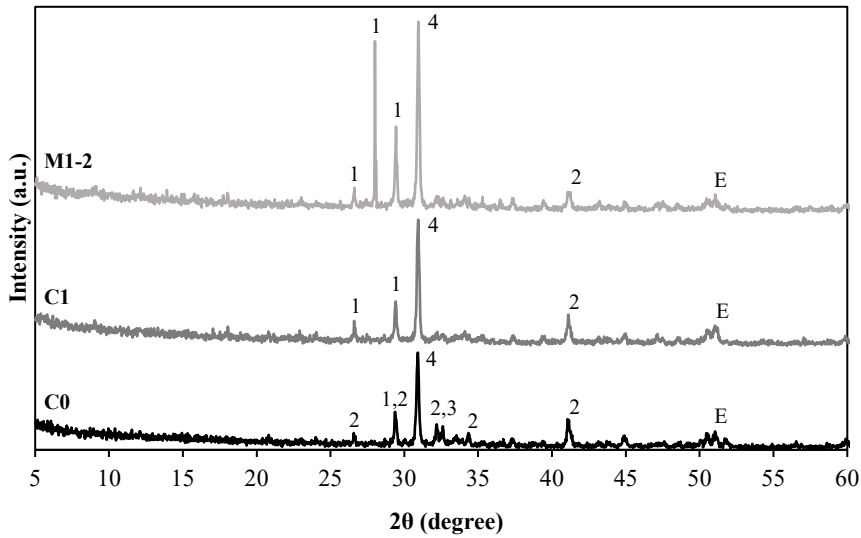


Figure 34: PXRD patterns of concrete at 1 day

Furthermore, to enhance the subsequent hydration reaction, spraying was applied to mix M4 (20a+4c-5P-6M). The PXRD patterns of the mix after spraying highlight a more intense C-S-H peak, which explains the 8% increase in compressive strength. Indeed, water spraying promoted the subsequent hydration reaction after carbonation, as reported in past research on the carbonation of Portland limestone cement [64]. Nevertheless, it is worth noting that the PXRD patterns of the carbonated mixes, regardless of carbonation parameters, identified C_3S and ettringite, indicating that these two compounds were not fully consumed during carbonation.

1: Calcite - CaCO_3 2: Tricalcium Silicate - C_3S 3: Dicalcium Silicate - C_2S
 4: Calcium Silicate Hydrate - C-S-H 5: Calcium Hydroxide - $\text{Ca}(\text{OH})_2$ A: Aragonite- CaCO_3
 E: Ettringite - $\text{Ca}_6\text{Al}_2(\text{SO}_4)_3(\text{OH})_{12}\cdot 26\text{H}_2\text{O}$

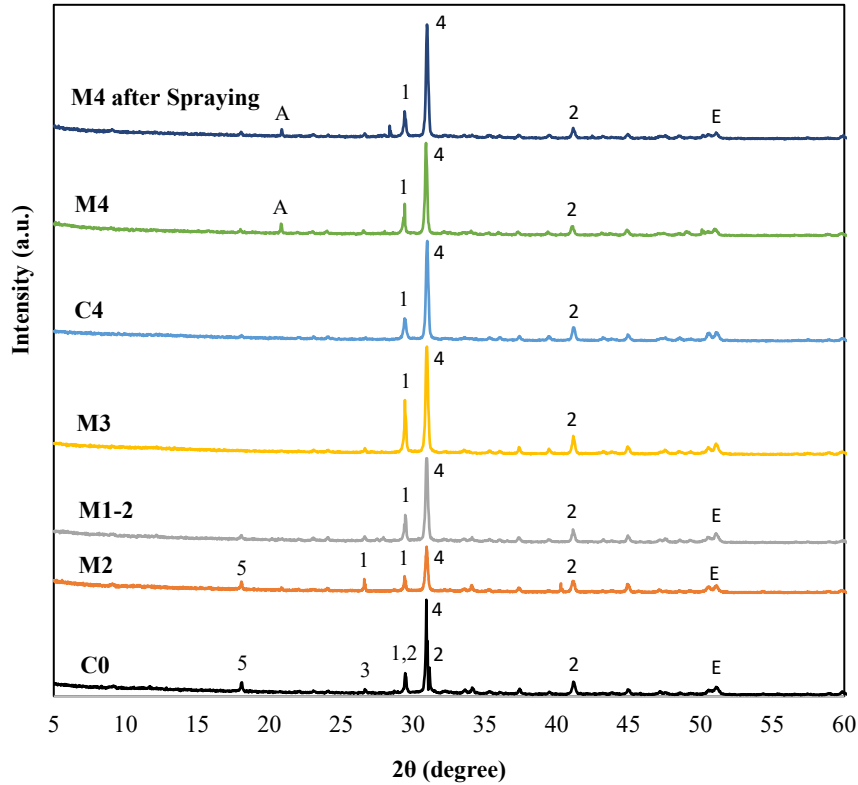


Figure 35: PXRD patterns of concrete at 28 days

4.2.2 Scanning Electron Microscope (SEM)

The morphological changes due to the carbonation curing parameters and incorporation of MOF in concrete were examined by SEM at the ages of 1 and 28 days. Energy dispersive X-ray (EDX) was used to analyze the morphology and identify the chemical compounds. Figure 36 shows the microstructure of a typical hydrated concrete at the age of 1 day. An intermix of the major hydration products was noted, including CH, ettringite, and C-S-H, in a relatively porous microstructure. It is worth noting that the detected CH did not resemble the typical hexagonal crystals (identified at 28 days), providing evidence of the formation of poorly crystalline CH, as noted in the PXRD earlier.

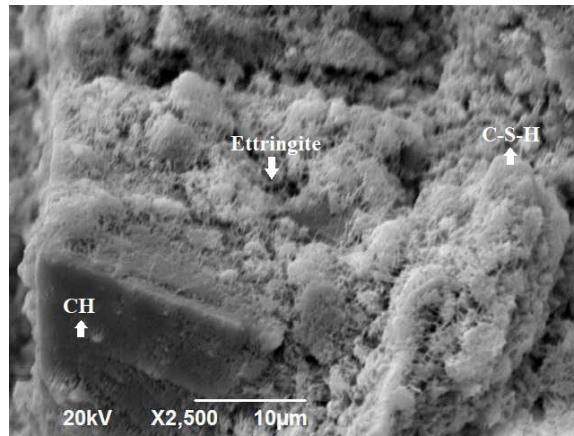


Figure 36: SEM of 1-day hydrated control mix C0

Furthermore, Figure 37 displays the micrograph of mix C1 (20a+4c-1P-0M). Similar to the control mix, ettringite and CH were found in the microstructure. Meanwhile, the C-S-H was intermixed with calcium carbonate (CaCO_3), as verified by the EDX spectrogram in Figure 38 and the PXRD patterns in Figure 34. Nevertheless, it is worth noting the CH detected in the SEM was not identified in the PXRD, possibly due to poor crystallinity, as noted in past work [117].

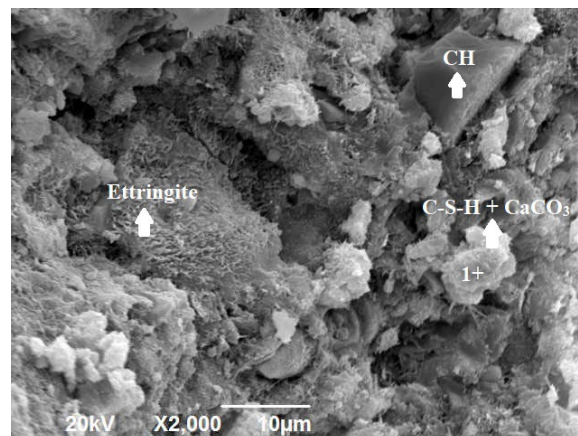


Figure 37: SEM of 1-day carbonated mix C1

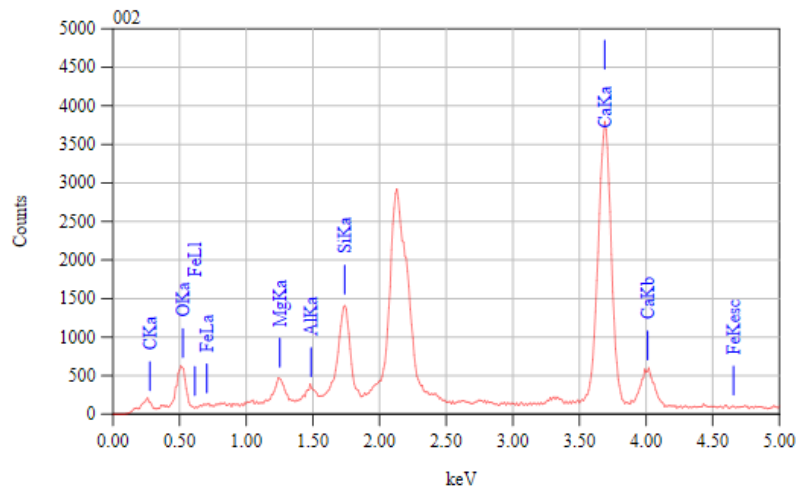


Figure 38: EDX analysis of point 1 in mix C1

The microstructure of the MOF-incorporating concrete M1-2 (20a+4c-1P-6M) is demonstrated in Figure 39. The NH₂-MIL-125 particles were spread across the microstructure. This was confirmed by the EDX spectrum in Figure 40, which clarifies the presence of titanium, one of the main elements of the MOF. Furthermore, an intermix of C-S-H and CaCO₃ was observed, which is aligned with the findings of the PXRD analysis. Compared to the counterpart without MOF, this intermix was more frequently noticed throughout the microstructure, albeit having a similarly dense structure.

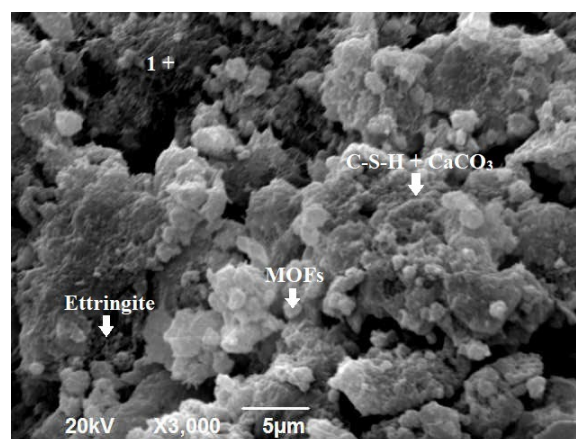


Figure 39: SEM of 1-day mix M1-2

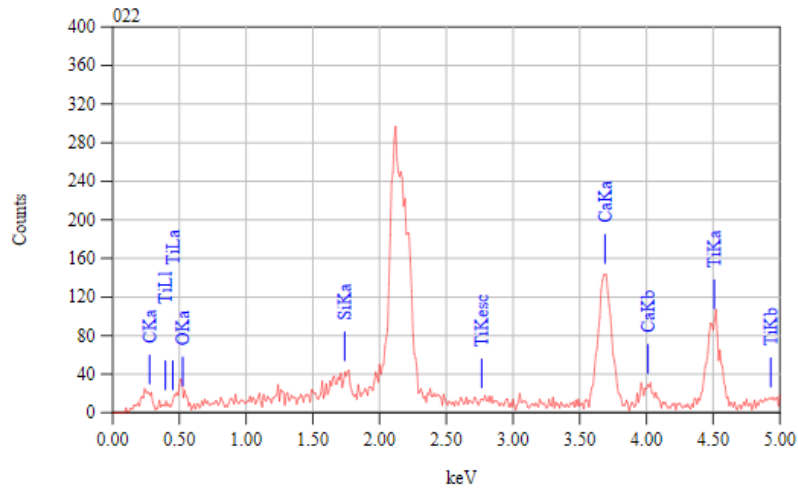


Figure 40: EDX analysis of point 1 in mix M1-2

Figure 41 illustrates the SEM micrograph of the hydrated control mix C0 at the age of 28 days. The image depicts the presence of more hydration products in the mix. The denser amorphous structure throughout the micrograph was attributed to the formation of C-S-H, whereas the hexagonal crystal indicated the presence of calcium hydroxide. Ettringite needles were also found to be incorporated in the calcium silicate hydrate gel.

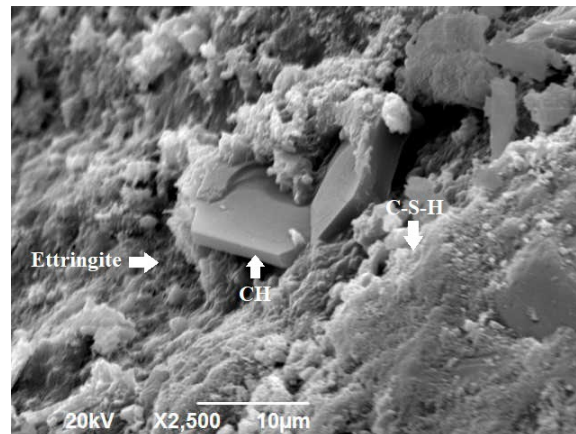


Figure 41: SEM of 28-day hydrated control mix C0

Incorporating MOF into the concrete had a significant impact on the microstructure. Comparing mixes C4 (Figures 42 and 43) and M4 (Figures 44 and 45) shows that the former has a more porous microstructure, owing to lower CO₂ uptake and, consequently,

lesser carbonation products. Clearly, the addition of MOF in mix M4 enhanced its CO₂ sequestration capacity, resulting in the further formation of calcite. Ettringite was unaffected by the addition of MOF, as it was noticed in the SEM morphology and PXRD phase analysis of C4 and M4. Also, calcium hydroxide was not present in either the SEM micrographs, owing to its reaction with carbon dioxide gas during the accelerated carbonation curing.

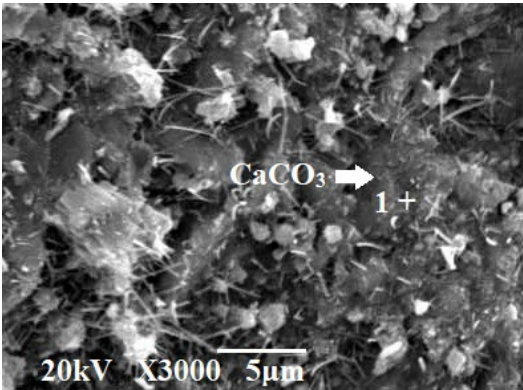


Figure 42: SEM of 28-day carbonated mix C4

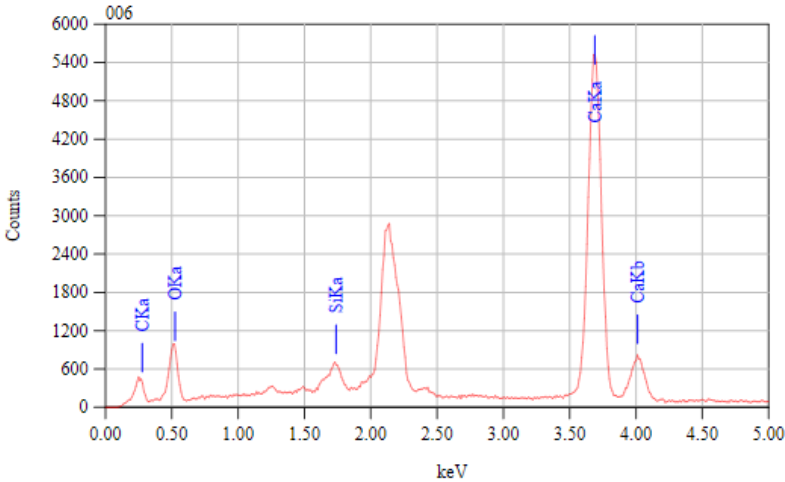


Figure 43: EDX analysis of point 1 in mix C4

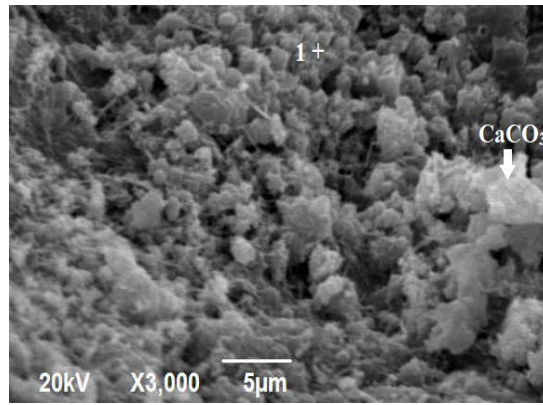


Figure 44: SEM of 28-day carbonated mix M4

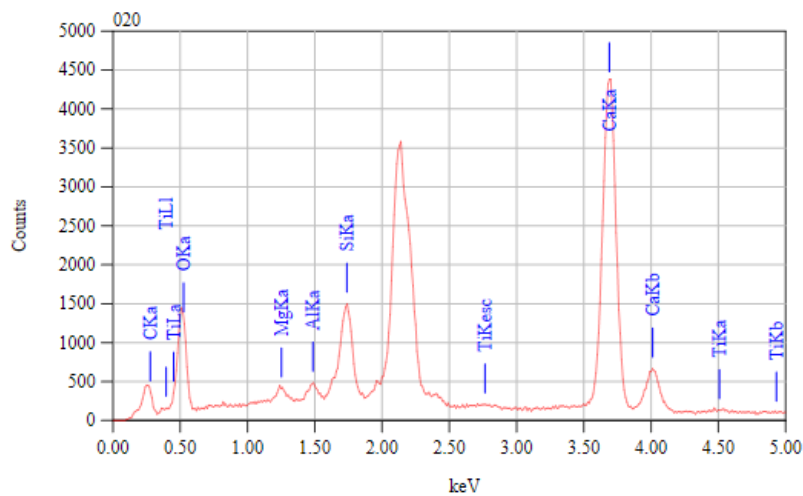


Figure 45: EDX analysis of point 1 in mix M4

The effect of initial curing duration on the microstructure was assessed by comparing mixes M2 (4a+4c-1P-6M) and M1-2 (20a+4c-1P-6M) in Figures 46 and 47, respectively. Mix M1-2 has a denser microstructure compared to M2, evidenced by the carbon uptake, compressive strength, and permeable pore voids volume test results. The evaporation of more free water caused by the extended initial curing duration promoted higher diffusion of CO₂ gas, hence more calcite precipitation (Figure 47). While the carbonation products occupied the majority of the micrograph of mix M1-2, the MOF particles were integrated with the CaCO₃, as evidenced by the titanium peak in the EDX analysis of Figure 48. It seems that the MOF particles acted as nucleation sites, thus promoting further carbonation of cement, and resulting in higher CO₂ uptake. Conversely, the MOF particles were visible in mix M2, owing to a less dense microstructure (Figure

46). Additionally, it can be observed that the ettringite needles were entangled with the calcium carbonate particles in both mixes. Meanwhile, calcium hydroxide was noted in mix M2 but was absent from mix M1-2, owing to its consumption due to carbonation, as verified by the PXRD patterns.

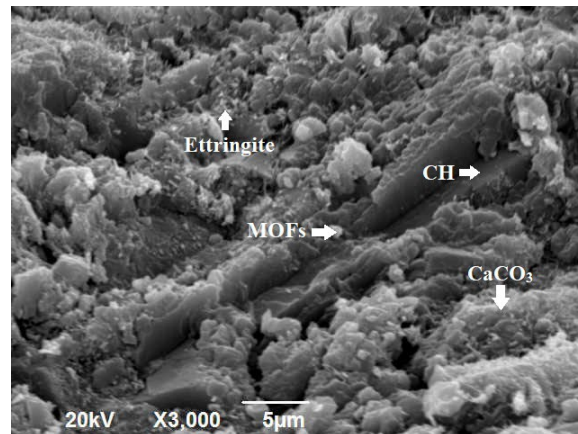


Figure 46: SEM of 28-day carbonated mix M2

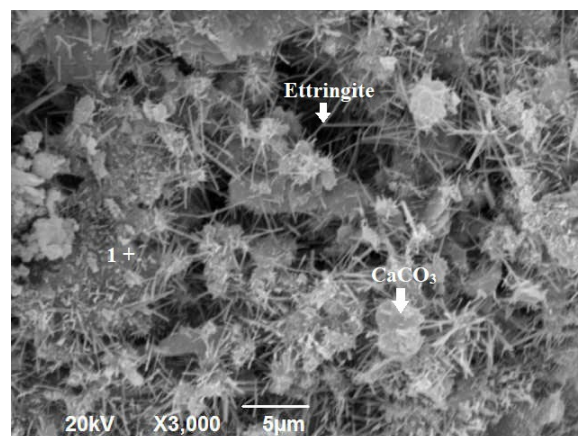


Figure 47: SEM of 28-day carbonated mix M1-2

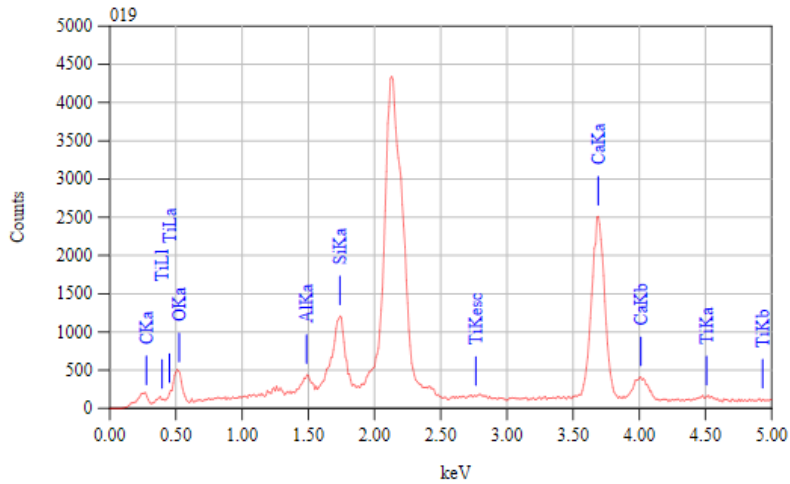


Figure 48: EDX analysis of point 1 in mix M1-2

Figure 49 illustrates the SEM micrograph of mix M3 (20a+20c-1P-6M) after 28 days. In comparison with mix M1-2 (20a+4c-1P-6M), mix M3 has a denser microstructure due to prolonged carbonation, which is consistent with the permeable pore voids volume findings. This also explains the higher compressive strength of mix M3 compared to M1-2. The MOF particles were not shown in the micrograph, as they were combined with CaCO_3 as appeared in the EDX analysis (Figure 50). This provides evidence of the MOFs' ability to act as nucleation sites for the additional formation of carbonation products, thereby increasing the CO_2 uptake.

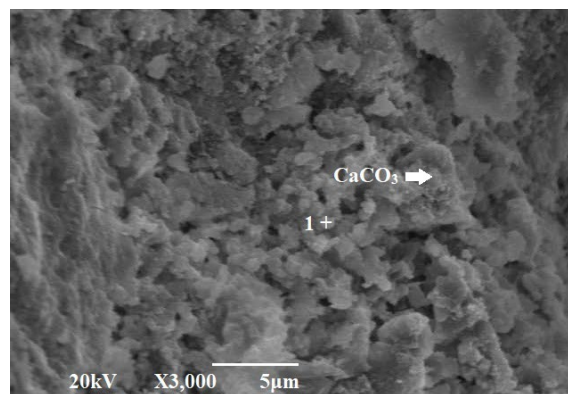


Figure 49: SEM of 28-day carbonated mix M3

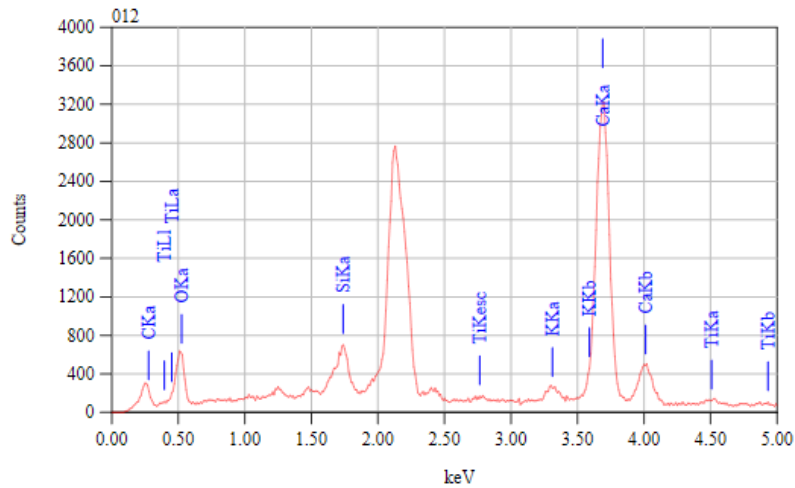


Figure 50: EDX analysis of point 1 in mix M3

The micrographs of mix M1-2 and M4 shed light on the influence of carbonation pressure on the microstructure of MOF-incorporating concrete. As demonstrated in Figure 44, the intermix of calcium carbonate and C-S-H dominated the microstructure of mix M4. Yet, MOF was incorporated within the carbonation reaction products, as shown in the EDX analysis in Figure 45. Higher pressure facilitated the diffusion of more CO₂ gas into the pores of the concrete, hence the precipitation of more carbonates, thus decreasing the porosity and void content of the mix.

Figure 51 displays the micrograph of 28-day concrete mix M4 after spraying. The post-carbonation spraying scheme led to densification in the microstructure due to the formation of more hydration products during the subsequent hydration, as illustrated in the PXRD patterns. Calcium silicate hydrate (C-S-H) along with closely packed calcium carbonate crystals are shown in Figure 51. Besides, the EDX analysis of Figure 52 assured the presence of MOF in the mix, despite its particles being hidden in a C-S-H/carbonate-dominant microstructure.

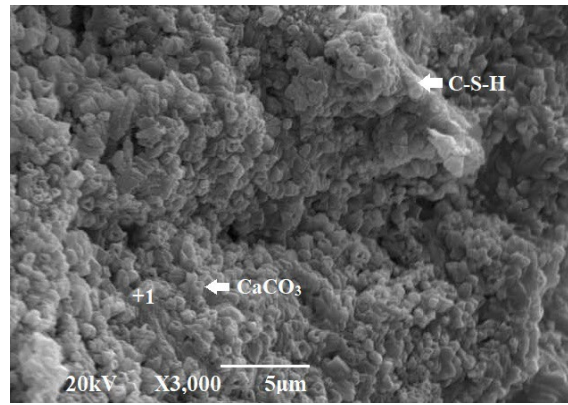


Figure 51: SEM of 28-day carbonated mix M4 after spraying

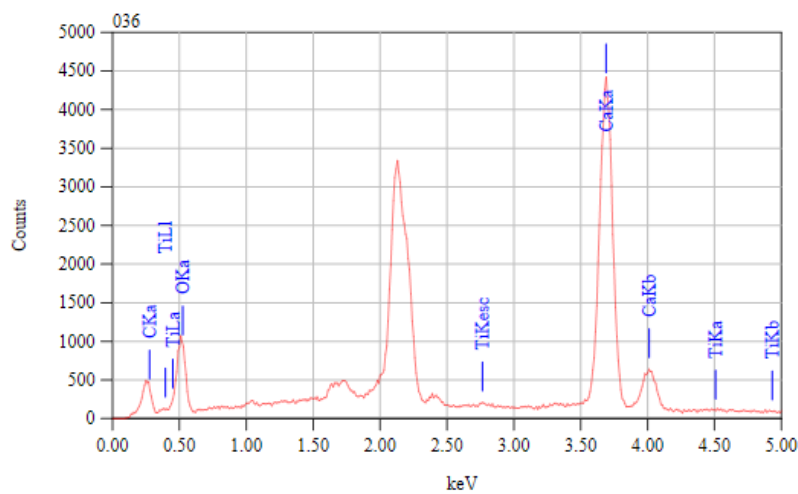


Figure 52: EDX analysis of point 1 in mix M4 after spraying

4.2.3 Fourier Transform Infrared (FTIR) Spectroscopy

Figures 53 and 54 show the results of the FTIR spectra of the 1-day and 28-day samples. The spectra are divided into seven zones. The band in the range of 3200-3600 cm^{-1} signified the stretching vibrations of H—OH groups, whereas 1600-1700 cm^{-1} related to the bending vibration of the O—H group. Meanwhile, the band at 1300-1500 cm^{-1} was associated with O—C—O in CO_3^{-2} groups, and the transmittance band in the range of 950-1000 cm^{-1} resembled the formation of C-S-H. In addition, bands at 800-875 cm^{-1} , 880-950 cm^{-1} , and 1000-1200 cm^{-1} represented the asymmetric stretching vibration of Si—O—T, where T is either Si or Al [30].

At the age of 1 day, the band at around 3640 cm^{-1} , originating from the O—H bond in the CH, existed in all mixes. As noted earlier, CH may not have been identified by PXRD due to poor crystallinity but was detected in the SEM micrographs. The strong absorption bands at 727 cm^{-1} , 876 cm^{-1} , and 1434 cm^{-1} , assigned to the CO_3^{2-} bending vibration in calcite, confirm the precipitation of calcium carbonate during carbon curing. However, in the reference hydrated mix C0, these peaks were owed to the presence of limestone aggregates in the mix, as indicated by the FTIR in Figure 3. Moreover, the vibrational bands at about 3440 cm^{-1} and 1630 cm^{-1} were caused by the vibration of the O—H group in the water. The intensity of the bands became stronger and sharper in mix C1 and M1-2, indicating a higher degree of reaction, thus the formation of more reaction products as evidenced by PXRD patterns.

Furthermore, in the 28-day samples (Figure 54), the band associated with the O—H bond in the CH at approximately 3642 cm^{-1} appeared in mixes C0 and M2 but became very weak or disappeared in other mixes as was noticed in the SEM morphology and PXRD phase analysis. However, incorporating MOF in mix M4 (20a+4c-5P-6M) resulting in stronger absorption bands for calcite at 728 cm^{-1} , 873 cm^{-1} and 1430 cm^{-1} than mix C4 (20a+4c-5P-0M). The addition of MOFs allowed the formation of more carbonation products which was verified by the SEM micrographs. Similarly, extending the initial curing and carbonation durations to 20 h for mixes M1-2 and M3, respectively, led to the precipitation of more carbonates and, hence, stronger bands than the counterpart mixes M2 and M1-2, correspondingly. The size of the diffraction peaks of calcite was obviously higher using 5 bars of pressure in mix M4 (20a+4c-5P-6M) compared to 1 bar in mix M1-2 (20a+4c-1P-6M), as noted in the PXRD analysis. Meanwhile, higher pressure also caused the formation of unstable carbonates, aragonite, which was detected at 857 cm^{-1} . Additionally, the post-carbonation spraying applied on mix M4 led to similar calcite peaks. Nevertheless, the water peaks were identified in all mixes at $3200\text{--}3600\text{ cm}^{-1}$. The intensity of the bands was slightly affected by the incorporation of MOFs in mix M4 compared to C4. However, these peaks became stronger with longer initial curing and carbonation. In the case of higher pressure, mix M4 (20a+4c-5P-6M) exhibited higher intensity of the band than mix M1-2 (20a+4c-1P-6M). Clearly, spraying the concrete mix M4 after the

carbonation process resulted in a stronger peak which indicated a higher degree of reaction, as illustrated in the SEM micrographs.

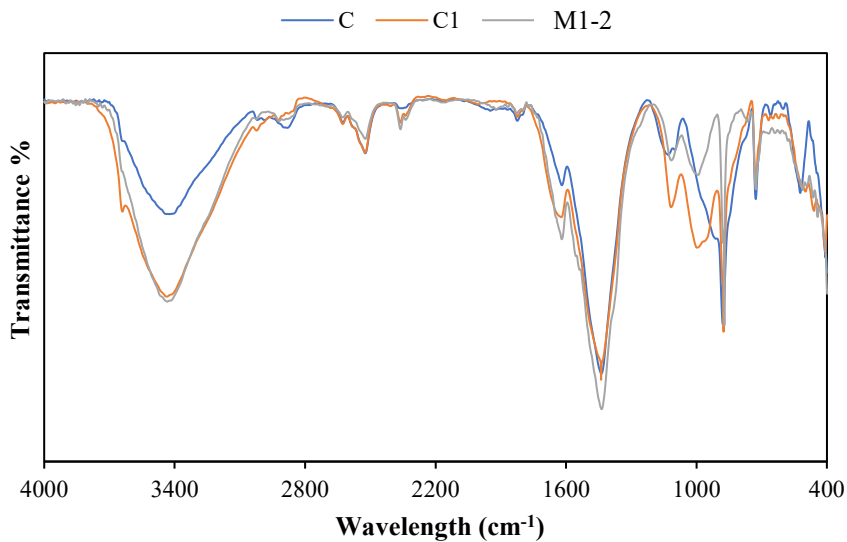


Figure 53: FTIR spectra of the 1-day samples

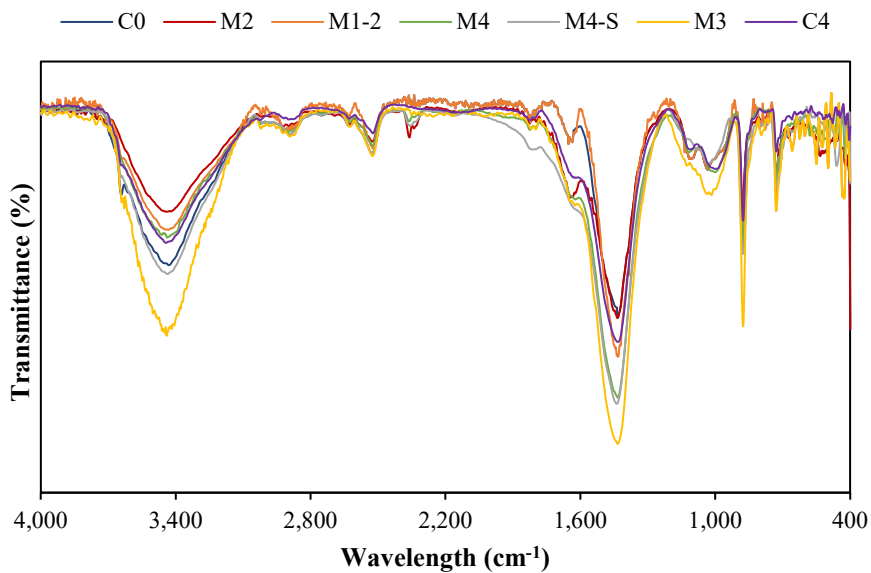


Figure 54: FTIR spectra of the 28-day samples

Chapter 5: Conclusion

5.1 Overview

The main purpose of this study was to develop sustainable and eco-friendly concrete that incorporates MOFs and utilizes accelerated carbonation curing to mitigate the CO₂ emissions resulting from the manufacture of cement. The potential use of MOFs as a main ingredient in the concrete was studied. Results showed that the proposed MOF-incorporating concrete has higher carbon sequestration capacity with superior mechanical and durability properties. Accordingly, this novel concrete product will have a lower impact on the environment while sufficing for the structural requirements of construction applications.

The experimental program comprises the selection and synthesis of the most suitable MOF that is capable of capturing CO₂. The ordinary Portland cement, aggregates, and water were characterized through extensive testing. Experiments were conducted to study the effect of different process parameters, including initial curing duration, carbonation duration, carbonation pressure, and quantity of MOF on the CO₂ uptake, mechanical properties, durability performance, and microstructure of concrete. Limitations and main findings of this thesis and recommendations for future studies are listed in this chapter.

5.2 Limitations of Work

The outcomes of this research study are limited to the specific concrete mixture constituents and proportions. Changing the mix design may cause a variation in the porosity of the concrete, which influences the diffusivity of the CO₂ gas, hence the CO₂ uptake. Also, other materials may have a different effect on the CO₂ uptake potential and concrete performance. Furthermore, the findings are limited to the specific MOF utilized in this work. In fact, incorporating another type of MOF with different CO₂ adsorption capacities may cause a variation in the CO₂ sequestration capacity. Additionally, the curing conditions adopted in this work mainly focused on carrying out the carbonation process within 24 hours, except for mixes C3 and M3, where the objective was to study the effect of prolonged initial curing and carbonation. As such, research findings presented herein

may not be generalized for mixes with curing durations beyond 40 hours (i.e., 20 hours of initial curing and 20 hours of carbonation).

5.3 Main Findings and Conclusions

MOFs have the capability to adsorb CO₂ gas, increase CO₂ uptake, and permanently sequester CO₂ gas within the concrete matrix. They have either improved or did not significantly affect the concrete performance. Based on the experimental results obtained in this thesis work, the following findings and conclusions can be drawn:

- Incorporating MOF in concrete up to 6%, by cement mass, led to an increase in CO₂ uptake up to 9.88% and carbonation depth to 6.8 mm in mix M1-2 (20a+4c-1P-6M). Increasing the quantity of MOF in the concrete mix caused a reduction in the carbonation reaction efficiency due to the possible agglomeration of MOF particles.
- The addition of MOF to the concrete promoted a higher degree of carbonation of cement, thus higher cement CO₂ uptake than that in mixes without MOF. However, the extent of improvement in the uptake was more pronounced with a longer initial curing duration and higher pressures.
- Prolonged initial curing had a more prominent impact on the degree of carbonation reaction and performance of concrete mixes incorporating MOF. Extending the duration from 4 to 20 hours increased the CO₂ uptake by 75% and carbonation depth by 48%. Meanwhile, the compressive strength increased by 125, 118, and 17% at 1, 7, and 28 days, while the water absorption and permeable pore voids volume were reduced by 9 and 5%, respectively.
- Extending carbonation curing of mixes incorporating 6% MOF led to higher CO₂ uptake, deeper carbonation depth, and enhanced compressive strength. The uptake and depth were improved by 93 and 71%, respectively, with the highest strength of 45.6 MPa compared to the carbonated control mix without MOF.
- Increasing the pressure during carbonation of MOF-incorporating mixes increased the carbon uptake by 50% and carbonation depth by 37%, but it had an insignificant effect on the compressive strength. Additionally, higher carbonation pressure reduced the water absorption and voids volume by 9 and 17%, correspondingly.

- The inclusion of MOF affected the early-age compressive strength, especially for mixes that had a short initial curing duration of 4 hours and high MOF content of 9%. This negative impact was reduced with subsequent hydration. Meanwhile, MOF-incorporating mixes had remarkable strength gain from 1 to 7 days compared to counterparts mixes without MOFs. This indicated that the addition of MOFs in concrete further accelerated the hydration reaction.
- Adding MOF beyond 6%, by cement mass, negatively affected the carbon uptake capacity and 1- and 7-day compressive strengths. However, this negative impact diminished over time. It may create more voids, resulting in higher water absorption and permeable pore voids volume.
- The optimum quantity of MOF, from an uptake and strength point of view, was 6%, by cement mass. For industries obliged to cure concrete for 24 hours at a pressure of 1 bar, the curing regime composed of 20-hour initial curing and 4-hour carbonation is optimum. The resultant CO₂ uptake and 28-day compressive strengths are 9.88% and 38.7 MPa, respectively. If a pressure of 5 bars could be employed, the respective parameters would be 14.78% and 39.9 MPa.
- The post-carbonation spraying technique reduced the water absorption and permeable voids of mix M4 by up to 2% and increased the strength by nearly 8%. Water spraying promoted the subsequent hydration reaction after carbonation, thus the formation of more hydration products, including C-S-H, and the densification of the microstructure.
- At the age of 1 day, the reaction products of the carbonated MOF-incorporating concrete M1-2 were C-S-H, calcite, and ettringite. The intermix of C-S-H and CaCO₃ was more frequently noticed throughout the microstructure of mix M1-2 compared to the counterparts mixes without MOF. The formation of ettringite needles in the mixes at 1 day was independent of the curing regime and presence of MOF. The calcium hydroxide peaks in the PXRD analysis were absent in all 1-day mixes, owing to the possible formation of poorly crystalline CH.
- Prolonging initial curing duration caused densification in the microstructure of mix M1-2. More calcite precipitated due to the evaporation of more free water and consumption of CH. Moreover, MOF particles were entangled with CaCO₃

particles. It seems that the MOF particles acted as nucleation sites, thus promoting further carbonation of cement and resulting in higher CO₂ uptake.

- Extending the carbonation curing duration led to a denser microstructure in mix M3 (20a+20c-1P-6M) compared to mix M1-2. More calcite and C-S-H were formed and combined with MOF particles. Meanwhile, an intermix of calcium carbonate and C-S-H dominated the microstructure of mix M4 (20a+4c-5P-6M) using 5 bars of pressure. Higher pressure facilitated the diffusion of more CO₂ gas, hence the precipitation of more carbonates. Also, unstable carbonates, aragonite, were formed in mix M4 carbonated at 5 bars pressure. The presence of MOF in the concrete mix may have contributed to maintaining the aragonite in its typical form.

5.4 Recommendations for Future Studies

Based on the main findings of this thesis work, the following are recommendations for future studies using MOF-incorporating concrete:

- Evaluate the CO₂ uptake and concrete performance of the same mix using various types of high CO₂ affinity MOFs.
- Investigate the impact of utilizing a MOF-incorporating concrete mix with different porosity on the carbon uptake capacity.
- Examine the CO₂ uptake, performance, and microstructure of MOF-incorporating concrete incorporating different binders, pozzolans, or SCMs in binary and ternary blends.
- Evaluate the long-term durability properties of MOF-incorporating concrete.
- Assess the effect of prolonging initial curing and carbonation durations beyond 40 hours on the CO₂ uptake and microstructure of concrete.
- Optimize the concrete mix proportions to maximize the CO₂ sequestration.
- Perform a lifecycle assessment analysis to verify the feasibility of using the MOF-incorporating concrete in the construction industry.

References

1. Miller, S.A., A. Horvath, and P.J. Monteiro, *Impacts of booming concrete production on water resources worldwide*. *Nature Sustainability*, 2018. 1(1): p. 69-76.
2. Imbabi, M.S., C. Carrigan, and S. McKenna, *Trends and developments in green cement and concrete technology*. *International Journal of Sustainable Built Environment*, 2012. 1(2): p. 194-216.
3. Pacheco-Torgal, F., et al., *Durability of alkali-activated binders: a clear advantage over Portland cement or an unproven issue?* *Construction and Building Materials*, 2012. 30: p. 400-405.
4. Andrew, R.M., *Global CO₂ emissions from cement production*. *Earth System Science Data*, 2018. 10(1): p. 195-217.
5. Mikulčić, H., M. Vujanović, and N. Duić, *Reducing the CO₂ emissions in Croatian cement industry*. *Applied energy*, 2013. 101: p. 41-48.
6. Ige, O.E., et al., *A review of the effectiveness of Life Cycle Assessment for gauging environmental impacts from cement production*. *Journal of Cleaner Production*, 2021: p. 129-213.
7. Gao, T., et al., *Analysis of material flow and consumption in cement production process*. *Journal of Cleaner Production*, 2016. 112: p. 553-565.
8. Mohamad, N., et al., *Environmental impact of cement production and Solutions: A review*. *Materials Today: Proceedings*, 2021. 48: p. 741-746
9. Gartner, E., *Industrially interesting approaches to "low-CO₂" cements*. *Cement and Concrete research*, 2004. 34(9): p. 1489-1498.
10. Yang, K.-H., et al., *Effect of supplementary cementitious materials on reduction of CO₂ emissions from concrete*. *Journal of Cleaner Production*, 2015. 103: p. 774-783.
11. Paris, J.M., et al., *A review of waste products utilized as supplements to Portland cement in concrete*. *Journal of Cleaner Production*, 2016. 121: p. 1-18.
12. AlArab, A., B. Hamad, and J.J. Assaad, *Strength and Durability of Concrete Containing Ceramic Waste Powder and Blast Furnace Slag*. *Journal of Materials in Civil Engineering*, 2022. 34(1): 04021392. doi: 10.1061/(ASCE)MT.1943-5533.0004031.
13. AlArab, A., et al., *Use of ceramic-waste powder as value-added pozzolanic material with improved thermal properties*. *Journal of Materials in Civil Engineering*, 2020. 32(9): 04020243. doi: 10.1061/(ASCE)MT.1943-5533.0003326.

14. El Mir, A., S.G. Nehme, and J.J. Assaad, *Durability of self-consolidating concrete containing natural waste perlite powders*. Heliyon, 2020. 6(1): e03165. doi: 10.1016/j.heliyon.2020.e03165.
15. Elia, H.N. and A.K. Akhnoukh, *Using Supplementary Cement Materials To reduce CO₂ Emissions From Cement Manufacturing*. International Journal of Engineering Research and Development 2018: p. 20-25
16. Flower, D.J. and J.G. Sanjayan, *Green house gas emissions due to concrete manufacture*. The international Journal of life cycle assessment, 2007. 12(5): p. 282-288.
17. Zhang, Y., et al. *Considering uncertainty in life-cycle carbon dioxide emissions of fly ash concrete*. in *Proceedings of the Institution of Civil Engineers-Engineering Sustainability*. Thomas Telford Ltd, 2018. 172(4): p. 198-206.
18. Muhedin, D., A. Jabar Hama Rash, and M. Hamakareem, *Sustainable Concrete by Using Fly ash as a Cement Replacement*. Second International Engineering Conference On Developments in Civil & Computer Engineering Applications 2016.
19. Tosti, L., et al., *Technical and environmental performance of lower carbon footprint cement mortars containing biomass fly ash as a secondary cementitious material*. Resources, Conservation and Recycling, 2018. 134: p. 25-33.
20. Van den Heede, P., et al., *Life cycle assessment of a column supported isostatic beam in high-volume fly ash concrete (HVFA concrete)*. 2nd International symposium on Service Life Design for Infrastructure, 2010: p. 437-444.
21. Crossin, E., *The greenhouse gas implications of using ground granulated blast furnace slag as a cement substitute*. Journal of Cleaner Production, 2015. 95: p. 101-108.
22. Feiz, R., et al., *Improving the CO₂ performance of cement, part I: utilizing life-cycle assessment and key performance indicators to assess development within the cement industry*. Journal of Cleaner Production, 2015. 98: p. 272-281.
23. Kim, Y., et al., *Slag waste incorporation in high early strength concrete as cement replacement: Environmental impact and influence on hydration & durability attributes*. Journal of Cleaner Production, 2018. 172: p. 3056-3065.
24. El-Hassan, H. and N. Ismail, *Effect of process parameters on the performance of fly ash/GGBS blended geopolymer composites*. Journal of Sustainable Cement-Based Materials, 2018. 7(2): p. 122-140.
25. El-Hassan, H., J. Medljy, and T. El-Maaddawy, *Properties of Steel Fiber-Reinforced Alkali-Activated Slag Concrete Made with Recycled Concrete Aggregates and Dune Sand*. Sustainability, 2021. 13(14): 8017. doi: 10.3390/su13148017.

26. El-Hassan, H., et al., *Performance of Steel Fiber-Reinforced Alkali-Activated Slag-Fly Ash Blended Concrete Incorporating Recycled Concrete Aggregates and Dune Sand*. Buildings, 2021. 11(8): 327. doi: 10.3390/buildings11080327.
27. El-Hassan, H., E. Shehab, and A. Al-Sallamin, *Effect of curing regime on the performance and microstructure characteristics of alkali-activated slag-fly ash blended concrete*. Journal of Sustainable Cement-Based Materials, 2021. 10(5): p. 289-317.
28. El-Hassan, H., E. Shehab, and A. Al-Sallamin, *Influence of different curing regimes on the performance and microstructure of alkali-activated slag concrete*. Journal of Materials in Civil Engineering, 2018. 30(9): 04018230. doi: 10.1061/(ASCE)MT.1943-5533.0002436.
29. Biricik, H., et al., *Activation of slag through a combination of NaOH/NaS alkali for transforming it into geopolymer slag binder mortar—assessment the effects of two different Blaine fines and three different curing conditions*. Journal of Materials Research and Technology, 2021. 14: p. 1569-1584.
30. El-Hassan, H. and S. Elkholy, *Performance Evaluation and Microstructure Characterization of Steel Fiber-Reinforced Alkali-Activated Slag Concrete Incorporating Fly Ash*. Journal of Materials in Civil Engineering, 2019. 31(10): 04019223. doi: 10.1061/(ASCE)MT.1943-5533.0002872.
31. El-Hassan, H. and S. Elkholy, *Enhancing the performance of alkali-activated slag-fly ash blended concrete through hybrid steel fiber reinforcement*. Construction and Building Materials, 2021. 311: p. 125-313.
32. Ismail, N. and H. El-Hassan, *Development and characterization of fly ash-Slag blended geopolymer mortar and lightweight concrete*. Journal of Materials in Civil Engineering, 2018. 30(4): 04018029. doi: 10.1061/(ASCE)MT.1943-5533.0002209.
33. Abu Obaida, F., T. El-Maaddawy, and H. El-Hassan, *Bond behavior of carbon fabric-reinforced matrix composites: Geopolymeric matrix versus cementitious mortar*. Buildings, 2021. 11(5): 207. doi: 10.3390/buildings11050207.
34. Hwalla, J., M. Saba, and J.J. Assaad, *Suitability of metakaolin-based geopolymers for underwater applications*. Materials and Structures, 2020. 53(5): p. 1-14.
35. Assaad, J.J. and M. Saba, *Suitability of Metakaolin-Based Geopolymers for Masonry Plastering*. ACI Materials Journal, 2020. 117(6): p. 269-279.
36. Najm, O., H. El-Hassan, and A. El-Dieb, *Optimization of alkali-activated ladle slag composites mix design using taguchi-based TOPSIS method*. Construction and Building Materials, 2022. 327: p. 126-946.
37. Najm, O., H. El-Hassan, and A. El-Dieb, *Ladle slag characteristics and use in mortar and concrete: A comprehensive review*. Journal of Cleaner Production, 2021. 288: p. 125-584.

38. Hassan, A., M. Arif, and M. Shariq, *Use of geopolymer concrete for a cleaner and sustainable environment—A review of mechanical properties and microstructure*. *Journal of cleaner production*, 2019. 223: p. 704-728.
39. Shi, X., et al., *Life Cycle Assessment and Impact Correlation Analysis of Fly Ash Geopolymer Concrete*. *Materials*, 2021. 14(23): p. 73-75.
40. Nguyen, L., et al., *Effects of composition and transportation logistics on environmental, energy and cost metrics for the production of alternative cementitious binders*. *Journal of Cleaner Production*, 2018. 185: p. 628-645.
41. Turner, L.K. and F.G. Collins, *Carbon dioxide equivalent (CO₂-e) emissions: A comparison between geopolymer and OPC cement concrete*. *Construction and building materials*, 2013. 43: p. 125-130.
42. McLellan, B.C., et al., *Costs and carbon emissions for geopolymer pastes in comparison to ordinary portland cement*. *Journal of cleaner production*, 2011. 19(9-10): p. 1080-1090.
43. Li, J., et al., *Green concrete containing diatomaceous earth and limestone: Workability, mechanical properties, and life-cycle assessment*. *Journal of cleaner production*, 2019. 223: p. 662-679.
44. HENDRICKS, C., *Emission Reduction of Greenhouse Gases from Cement Industry, 2004*. IEA Greenhouse Gas R & D Programme, 2017: p. 939-944
45. Ali, M., R. Saidur, and M. Hossain, *A review on emission analysis in cement industries*. *Renewable and Sustainable Energy Reviews*, 2011. 15(5): p. 2252-2261.
46. Aranda-Usón, A., et al., *Characterisation and environmental analysis of sewage sludge as secondary fuel for cement manufacturing*. *Chemical Engineering Transactions*, 2012. 29: p. 457-462.
47. Kaddatz, K., M. Rasul, and A. Rahman, *Alternative fuels for use in cement kilns: process impact modelling*. *Procedia Engineering*, 2013. 56: p. 413-420.
48. Rahman, A., et al., *Assessment of energy performance and emission control using alternative fuels in cement industry through a process model*. *Energies*, 2017. 10(12): 1996. doi: 10.3390/en10121996.
49. Wojtacha-Rychter, K., P. Kucharski, and A. Smolinski, *Conventional and Alternative Sources of Thermal Energy in the Production of Cement—An Impact on CO₂ Emission*. *Energies*, 2021. 14(6): 1539. doi: 10.3390/en14061539.
50. Bourtsalas, A.C.T., et al., *Use of non-recycled plastics and paper as alternative fuel in cement production*. *Journal of cleaner production*, 2018. 181: p. 8-16.
51. Hossain, M.U., et al., *Techno-environmental feasibility of wood waste derived fuel for cement production*. *Journal of Cleaner Production*, 2019. 230: p. 663-671.

52. Fyffe, J.R., et al., *Use of MRF residue as alternative fuel in cement production*. Waste management, 2016. 47: p. 276-284.
53. Ahmed, U. and U. Zahid, *Techno-economic assessment of future generation IGCC processes with control on greenhouse gas emissions*, in *Computer Aided Chemical Engineering*. 2019, Elsevier. p. 529-534.
54. Zhou, W., et al., *Capturing CO₂ from cement plants: A priority for reducing CO₂ emissions in China*. Energy, 2016. 106: p. 464-474.
55. An, J., R.S. Middleton, and Y. Li, *Environmental Performance Analysis of Cement Production with CO₂ Capture and Storage Technology in a Life-Cycle Perspective*. Sustainability, 2019. 11(9): 2626. doi: 10.3390/su11092626.
56. Barker, D., et al., *CO₂ capture in the cement industry*. Energy procedia, 2009. 1(1): p. 87-94.
57. Osman, D.A.M., O. Nur, and M.A. Mustafa, *Reduction of energy consumption in cement industry using zinc oxide nanoparticles*. Journal of Materials in Civil Engineering, 2020. 32(6): 04020124. doi: 10.1061/(asce)mt.1943-5533.0003196.
58. Cosentino, I., et al., *Nano CaCO₃ particles in cement mortars towards developing a circular economy in the cement industry*. Procedia Structural Integrity, 2020. 26: p. 155-165.
59. Moro, C., V. Francioso, and M. Velay-Lizancos, *Impact of nano-TiO₂ addition on the reduction of net CO₂ emissions of cement pastes after CO₂ curing*. Cement and Concrete Composites, 2021. 123: 104160. doi: 10.1016/j.cemconcomp.2021.104160.
60. Shao, Y. and H. El-Hassan, *CO₂ utilization in concrete*. Third International Conference on Sustainable Construction Materials and Technologies (SCMT3), 2013.
61. Shi, C., et al., *Accelerated carbonation as a fast curing technology for concrete blocks*. Sustainable and nonconventional construction materials using inorganic bonded fiber composites, 2017: p. 313-341.
62. El-Hassan, H., *Accelerated Carbonation Curing as a Means of Reducing Carbon Dioxide Emissions*, in *Cement Industry-Optimization, Characterization and Sustainable Application*. 2020, IntechOpen. doi: 10.5772/intechopen.93929
63. El-Hassan, H., Y. Shao, and Z. Ghoulch, *Effect of Initial Curing on Carbonation of Lightweight Concrete Masonry Units*. ACI Materials Journal, 2013. 110(4): p. 441-450.
64. El-Hassan, H. and Y. Shao, *Early carbonation curing of concrete masonry units with Portland limestone cement*. Cement and Concrete Composites, 2015. 62: p. 168-177.

65. El-Hassan, H., Y. Shao, and Z. Ghoulleh, *Reaction products in carbonation-cured lightweight concrete*. Journal of materials in civil engineering, 2013. 25(6): p. 799-809.
66. El-Hassan, H. and Y. Shao, *Dynamic carbonation curing of fresh lightweight concrete*. Magazine of concrete research, 2014. 66(14): p. 708-718.
67. Yang, X. and X.-Y. Wang, *Strength and durability improvements of biochar-blended mortar or paste using accelerated carbonation curing*. Journal of CO₂ Utilization, 2021. 54: 101766. doi: 10.1016/j.jcou.2021.101766.
68. Wu, H.-L., et al., *Development of reactive MgO-based Engineered Cementitious Composite (ECC) through accelerated carbonation curing*. Construction and Building Materials, 2018. 191: p. 23-31.
69. Zhang, D., X. Cai, and Y. Shao, *Carbonation curing of precast fly ash concrete*. Journal of Materials in Civil Engineering, 2016. 28(11): 04016127. doi: 10.1061/(ASCE)MT.1943-5533.0001649.
70. Qin, L., X. Gao, and T. Chen, *Influence of mineral admixtures on carbonation curing of cement paste*. Construction and Building Materials, 2019. 212: p. 653-662.
71. Park, B. and Y.C. Choi, *Effect of Carbonation Curing on Physical and Durability Properties of Cementitious Materials Containing AOD Slag*. Applied Sciences, 2020. 10(19): 6646. doi: 10.3390/app10196646.
72. Dixit, A., H. Du, and S. Dai Pang, *Carbon capture in ultra-high performance concrete using pressurized CO₂ curing*. Construction and Building Materials, 2021. 288: 123076. doi: 10.1016/j.conbuildmat.2021.123076.
73. Mo, L. and D.K. Panesar, *Effects of accelerated carbonation on the microstructure of Portland cement pastes containing reactive MgO*. Cement and Concrete Research, 2012. 42(6): p. 769-777.
74. Phung, Q.T., et al., *Effect of limestone fillers on microstructure and permeability due to carbonation of cement pastes under controlled CO₂ pressure conditions*. Construction and Building Materials, 2015. 82: p. 376-390.
75. Seo, J.H., et al., *CO₂ uptake of carbonation-cured cement blended with ground volcanic ash*. Materials, 2018. 11(11): 2187. doi: 10.3390/ma11112187.
76. Qin, L. and X. Gao, *Properties of coal gangue-Portland cement mixture with carbonation*. Fuel, 2019. 245: p. 1-12.
77. Qin, L. and X. Gao, *Recycling of waste autoclaved aerated concrete powder in Portland cement by accelerated carbonation*. Waste Management, 2019. 89: p. 254-264.

78. Mo, L. and D.K. Panesar, *Accelerated carbonation—A potential approach to sequester CO₂ in cement paste containing slag and reactive MgO*. Cement and Concrete Composites, 2013. 43: p. 69-77.
79. Hameed, R., et al., *CO₂ Uptake and Physicochemical Properties of Carbonation-Cured Ternary Blend Portland Cement–Metakaolin–Limestone Pastes*. Materials, 2020. 13(20): 4656. doi: 10.3390/ma13204656.
80. Liu, Y., Z.U. Wang, and H.C. Zhou, *Recent advances in carbon dioxide capture with metal-organic frameworks*. Greenhouse Gases: Science and Technology, 2012. 2(4): p. 239-259.
81. Sumida, K., et al., *Carbon dioxide capture in metal–organic frameworks*. Chemical reviews, 2012. 112(2): p. 724-781.
82. Li, P., et al., *Water stability and competition effects toward CO₂ adsorption on metal organic frameworks*. Separation & Purification Reviews, 2015. 44(1): p. 19-27.
83. Soni, S., P.K. Bajpai, and C. Arora, *A review on metal-organic framework: synthesis, properties and application*. Characterization and Application of Nanomaterials, 2020. 3(2): p. 87-106.
84. Aniruddha, R., I. Sreedhar, and B.M. Reddy, *MOFs in carbon capture—past, present and future*. Journal of CO₂ Utilization, 2020. 42: 101297. doi: 10.1016/j.jcou.2020.101297.
85. Thiruvenkatachari, R., et al., *Post combustion CO₂ capture by carbon fibre monolithic adsorbents*. Progress in Energy and Combustion Science, 2009. 35(5): p. 438-455.
86. Elhenawy, S.E.M., et al., *Metal-organic frameworks as a platform for CO₂ capture and chemical processes: Adsorption, membrane separation, catalytic-conversion, and electrochemical reduction of CO₂*. Catalysts, 2020. 10(11): 1293. doi: 10.3390/catal10111293.
87. Zhang, Z., et al., *Perspective of microporous metal–organic frameworks for CO₂ capture and separation*. Energy & environmental science, 2014. 7(9): p. 2868-2899.
88. Martínez, F., et al., *Amino-impregnated MOF materials for CO₂ capture at post-combustion conditions*. Chemical Engineering Science, 2016. 142: p. 55-61.
89. Babarao, R. and J.W. Jiang, *Cation characterization and CO₂ capture in Li⁺-exchanged metal– organic frameworks: From first-principles modeling to molecular simulation*. Industrial & engineering chemistry research, 2011. 50(1): p. 62-68.
90. Carpenter, S.M. and H.A. Long Iii, *Integration of carbon capture in IGCC systems, in Integrated Gasification Combined Cycle (IGCC) Technologies*. 2017, Elsevier. p. 445-463.

91. Günther, C., M. Weng, and A. Kather, *Restrictions and limitations for the design of a steam generator for a coal-fired oxyfuel power plant with circulating fluidised bed combustion*. Energy procedia, 2013. 37: p. 1312-1321.
92. Ahmad, S., et al., *Effects of carbonation pressure and duration on strength evolution of concrete subjected to accelerated carbonation curing*. Construction and Building Materials, 2017. 136: p. 565-573.
93. Astm, C., *Standard Specification for Portland Cement, ASTM International*. 2020. doi: 10.1520/C0150-05.
94. Astm, C., *Standard specification for concrete aggregates*. Philadelphia, PA: American Society for Testing and Materials, 2003. doi: 10.1520/C0033-07.
95. American Society for Testing and, M., *ASTM C 1602 standard specification for mixing water used in the production of hydraulic cement concrete*. 2006. doi: 10.1520/C1602_C1602M-12.
96. Astm, C., *136. Standard test method for sieve analysis of fine and coarse aggregates*. American Society for Testing and Materials, Philadelphia, PA, 2005. doi: 10.1520/C0136-06.
97. a, A.C.C.M., *Standard test method for bulk density ("unit weight") and voids in aggregate*. 2017, American Society for Testing and Materials Philadelphia, PA, USA. doi: 10.1520/C0029_C0029M-17A.
98. Astm, A., *Standard test method for relative density (specific gravity) and absorption of coarse aggregate*. ASTM West Conshohocken, PA, 2015. doi: 10.1520/C0127-15.
99. Kim, S.-N., et al., *Adsorption/catalytic properties of MIL-125 and NH₂-MIL-125*. Catalysis today, 2013. 204: p. 85-93.
100. Muelas-Ramos, V., et al., *Synthesis of noble metal-decorated NH₂-MIL-125 titanium MOF for the photocatalytic degradation of acetaminophen under solar irradiation*. Separation and Purification Technology, 2021. 272: 118896. doi: 10.1016/j.seppur.2021.118896.
101. Kaur, M., S.K. Mehta, and S.K. Kansal, *Amine-functionalized titanium metal-organic framework (NH₂-MIL-125 (Ti)): A novel fluorescent sensor for the highly selective sensing of copper ions*. Materials Chemistry and Physics, 2020. 254: p. 123-539.
102. Astm, C., *Standard practice for making and curing concrete test specimens in the laboratory (ASTM C192)*. 2016. doi: 10.1520/C0192_C0192M-16.
103. El-Hassan, H. and Y. Shao, *Carbon storage through concrete block carbonation curing*. Journal of Clean Energy Technologies, 2014. 2(3): p. 287-291.
104. Bsi, *BS EN 12390-3: 2009: Testing hardened concrete. Compressive strength of test specimens*. 2009, BSI London, UK. doi: 10.3403/BSEN12390.

105. C642-13, A., *Standard test method for density, absorption, and voids in hardened concrete*. West Conshohocken, PA: ASTM International, 2013. doi: 10.1520/C0642-13
106. Zhao, X., et al., *NH₂-MIL-125 (Ti)/TiO₂ composites as superior visible-light photocatalysts for selective oxidation of cyclohexane*. *Molecular Catalysis*, 2018. 452: p. 175-183.
107. Sohail, M., et al., *Synthesis of highly crystalline NH₂-MIL-125 (Ti) with S-shaped water isotherms for adsorption heat transformation*. *Crystal Growth & Design*, 2017. 17(3): p. 1208-1213.
108. Tu, Z., C. Shi, and N. Farzadnia, *Effect of limestone powder content on the early-age properties of CO₂-cured concrete*. *Journal of Materials in Civil Engineering*, 2018. 30(8): 04018164. doi: 10.1061/(ASCE)MT.1943-5533.0002232.
109. Sharma, D. and S. Goyal, *Accelerated carbonation curing of cement mortars containing cement kiln dust: An effective way of CO₂ sequestration and carbon footprint reduction*. *Journal of Cleaner Production*, 2018. 192: p. 844-854.
110. Mo, L., et al., *Effectiveness of using CO₂ pressure to enhance the carbonation of Portland cement-fly ash-MgO mortars*. *Cement and Concrete Composites*, 2016. 70: p. 78-85.
111. Xian, X. and Y. Shao, *Microstructure of cement paste subject to ambient pressure carbonation curing*. *Construction and Building Materials*, 2021. 296: 123652. doi: 10.1016/j.conbuildmat.2021.123652.
112. Xian, X. and Y. Shao, *Carbonation curing of concretes in a flexible enclosure under ambient pressure*. *Journal of Materials in Civil Engineering*, 2021. 33(4): 04021025. doi: 10.1061/(ASCE)MT.1943-5533.0003648.
113. Poon, C.S., Z.H. Shui, and L. Lam, *Effect of microstructure of ITZ on compressive strength of concrete prepared with recycled aggregates*. *Construction and building materials*, 2004. 18(6): p. 461-468.
114. Vargas, P., O. Restrepo-Baena, and J.I. Tobón, *Microstructural analysis of interfacial transition zone (ITZ) and its impact on the compressive strength of lightweight concretes*. *Construction and Building Materials*, 2017. 137: p. 381-389.
115. Maddalena, R., et al., *Direct synthesis of a solid calcium-silicate-hydrate (CSH)*. *Construction and Building Materials*, 2019. 223: p. 554-565.
116. Mohsen, A., et al., *Evaluating the mechanical properties of admixed blended cement pastes and estimating its kinetics of hydration by different techniques*. *Egyptian Journal of Petroleum*, 2020. 29(2): p. 171-186.
117. Berger, R.L. and J.D. McGregor, *Effect of Temperature and Water-Solid Ratio on Growth of Ca(OH)₂ Crystals Formed During Hydration of Ca₃SiO₅*. *Journal of the American Ceramic Society*, 1973. 56(2): p. 73-79.

118. Park, S., et al., *Reaction of hydrated cement paste with supercritical carbon dioxide*. Construction and Building Materials, 2021. 281: 122615. doi: 10.1016/j.conbuildmat.2021.122615.



جامعة الإمارات العربية المتحدة
United Arab Emirates University



UAE UNIVERSITY MASTER THESIS NO. 2022: 36

This thesis evaluates the feasibility of using metal-organic frameworks (MOFs) in concrete to curb the CO₂ emissions from the production of cement. The CO₂ uptake, mechanical properties, durability, and microstructure characteristics of MOF-incorporating concrete were evaluated. The study revealed that the addition of MOFs promoted a higher carbonation degree of cement, especially with a longer initial curing duration and higher pressures. Incorporating up to 6% MOF, by cement mass, resulted in superior carbon sequestration potential. Microstructure analysis highlighted the formation of calcite and calcium silicate hydrate. The developed MOF-incorporating concrete can be used in construction applications to mitigate the industry-related CO₂ emissions with either improve or not significantly affect the concrete properties.

Mona Ibrahim El-Hallak has received her Master of Science in Civil and Environmental Engineering from the Department of Civil and Environmental Engineering, College of Engineering at UAE University, UAE. She has received her BSc from the College of Engineering, UAE University, UAE.

www.uaeu.ac.ae

UAEU عمادة المكتبات
Libraries Deanship

جامعة الإمارات العربية المتحدة
United Arab Emirates University



قسم الخدمات المكتبية الرقمية - Digital Library Services Section